Accepted Manuscript

Geological Society, London, Memoirs

Eurasia Basin Composite Tectono-Sedimentary Element

J. I. Faleide, M. M. Abdelmalak, A. Minakov, J. C. Meza-Cala, A. P. E. Lasabuda, C. Gaina & S. Drachev

DOI: https://doi.org/10.1144/M57-2023-16

To access the most recent version of this article, please click the DOI URL in the line above. When citing this article please include the above DOI.

Received 19 September 2023
Revised 5 April 2024
Accepted 13 April 2024

Eurasia Basin Composite Tectono-Sedimentary Element

Faleide, J. I.[1], Abdelmalak, M. M.[1], Minakov, A.[1,2], Meza-Cala, J. C.[1,2],

Lasabuda, A. P. E.[1,2,3], Gaina, C.[1,2], Drachev, S.[4]

[1]Department of Geosciences, University of Oslo, Norway

[2]Centre for Planetary Habitability (PHAB), Department of Geosciences, University of Oslo, Norway

[3]Earlier at Department of Geosciences, UiT-The Arctic University of Norway, Tromsø, Norway

[4]ArcGeoLink Ltd, 2 Harestone Valley Road, Caterham CR3 6HB, Surrey, UK

Corresponding author: Jan Inge Faleide, j.i.faleide@geo.uio.no

Abstract

The Eurasia Basin formed by continental breakup and separation of the Lomonosov Ridge from the northern Barents-Kara shelves at about 54-56 Ma. It was a restricted oceanic basin since its formation until the Miocene, when extensive water circulation between the North Atlantic and Arctic commenced through the Fram Strait gateway. The opening of the oceanic gateway had large impact on paleoceanography and paleoclimate, which evolved from an Eocene greenhouse to a Neogene icehouse associated with northern hemisphere glaciations. The Eocene to present sedimentary fill of the Eurasia Basin was mainly sourced from surrounding shelf areas in the Barents, Kara and Laptev seas, which experienced widespread Cenozoic uplift and erosion during several phases. The stratigraphy of the Eurasia Basin is poorly constrained due to lack of boreholes penetrating the basin fill. We therefore have to rely on seismic stratigraphy and tentative ages assigned to sequences and their boundaries terminating on top of oceanic basement of known age. This contribution covers two tectono-sedimentary elements (TSE), the Eurasia Basin Oceanic TSE and the Eurasia Basin Prograded Margin TSE, which are closely connected and difficult to draw a distinct boundary between.

Introduction

The Eurasia Basin is the youngest actively spreading oceanic basin in the Arctic Ocean between diverging North American and Eurasian lithospheric plates (Fig. 1A). It formed as a result of breakup and separation of the Lomonosov Ridge from the northern Barents-Kara shelves at about 54-56 Ma (Kristoffersen *et al.* 1990; Glebovsky *et al.* 2006; Nikishin *et al.* 2018, 2021b). The conjugate margins are characterized by a narrow zone of crustal thinning from the continent to the ocean (Minakov *et al.* 2012; Funck *et al.* 2022).

The present plate boundary, the Gakkel Ridge, separates the Nansen and Amundsen basins (Fig. 1). The ridge is characterized by ultraslow full spreading rates varying from ~13 mm/year in the west to ~6 mm/year in the east (Brozena *et al*. 2003; Glebovsky *et al.* 2006; Gaina *et al.* 2015; Nikishin *et al.* 2018; Jokat *et al*. 2019). The spreading rate decreases towards the Laptev Sea margin where the plate boundary continues into the continent (Drachev *et al.* 2003, 2018, 2024a; Engen *et al.* 2003; Drachev and Shkarubo 2018).

The Eurasia Basin was a restricted oceanic basin since its formation until the Miocene, sometime between 20 and 15 Ma (Jakobsson *et al.* 2007; Engen *et al.* 2008; Jokat *et al.* 2016), when extensive water circulation between the North Atlantic and Arctic commenced through the Fram Strait gateway. The opening of the oceanic gateway had large impact on paleoceanography and paleoclimate, which evolved from an Eocene greenhouse to a Neogene icehouse associated with northern hemisphere glaciations (Smith and Pickering 2003; Hutchinson *et al.* 2019; Stein 2019).

The Eocene to present sedimentary fill of the Eurasia Basin was mainly sourced from the surrounding shelves, which experienced widespread Cenozoic uplift and erosion during several phases (Dimakis *et al.* 1998; Sekretov 2002; Henriksen *et al.* 2011; Lasabuda *et al.* 2018, 2021; Piskarev *et al*. 2018; Shipilov *et al*. 2021; Medvedev *et al.* 2022).

The Eurasia Basin stratigraphy is poorly constrained due to lack of boreholes and rather scarce grid of regional 2D multichannel seismic reflection (MCS) profiles. We therefore have to rely on seismic stratigraphy and tentative ages assigned to sequences and their boundaries terminating against the oceanic basement of known age (see below). The lack of boreholes in the Eurasia Basin also makes it difficult to assess its petroleum potential (Moore and Pitman 2011).

In this chapter, we represent the Eurasia Basin's sedimentary fill as a composite tectono-sedimentary element (CTSE) consisting of two individual TSEs: (i) an oceanic basin TSE and (ii) a prograded margin TSE. These sedimentary bodies are closely interlinked via facies changes and, therefore, are difficult to divide.

Age

The Eurasia Basin CTSE has an inferred Eocene to present age (Fig. 2). It lacks direct age datings; therefore its age is based on correlations with distant scientific boreholes in the surrounding regions and the interpreted age of underlying oceanic crust. The ACEx borehole on the Lomonosov Ridge reached uppermost Cretaceous strata (Backman *et al.* 2005, 2008; Moran *et al.* 2006a,b) and ODP boreholes on the SW Yermak Plateau penetrated Plio-Pleistocene strata (Myhre *et al.* 1995; Grøsfjeld *et al.* 2014; Knies *et al.* 2014; Mattingsdal *et al*. 2014) (Figs. 1B and 2).

Geographic location and dimensions

The Eurasia Basin is about 2000 km long and 500-700 km wide. It is narrower (~300 km) in the western part, bounded by the conjugate Yermak Plateau and Morris Jesup Rise (Fig. 1B). The oceanic Eurasia Basin is surrounded by the wide Barents-Kara and Laptev shelves in the south and east respectively. It is separated from the older Amerasia Basin by the Lomonosov Ridge, a continental sliver split off the Barents-Kara shelf (Jokat *et al.* 1995b; Brozena *et al.* 2003; Minakov *et al.* 2012; Piskarev *et al.* 2019; Abdelmalak *et al.* 2023; Kristoffersen *et al.* 2022). Towards North Greenland the Amundsen Basin part of the Eurasia Basin is bounded by the Lincoln Sea and Morris Jesup Rise (Jokat *et al.* 1995a; Døssing *et al.* 2014; Kristoffersen *et al.* 2021). The oceanic TSE is extended into the Fram Strait, where the Gakkel Ridge links up with the Lena Trough (Fig. 1B), which is characterized by oblique sparsely magmatic seafloor spreading (Snow *et al.* 2011; Laukert *et al.* 2014; Jokat *et al.* 2016). North of Svalbard, the Nansen Basin part of the TSE is bounded by the Sophia Basin and Yermak Plateau (Fig. 1B; Geissler and Jokat 2004; Jokat *et al.* 2008; Geissler *et al.* 2011; Kristoffersen *et al.* 2020). The Sophia Basin and the corresponding basin in the Lincoln Sea (Fig. 1B) were closely linked to the initial opening of the Eurasia Basin.

Principal data sets

Wells

No exploration wells or deep scientific boreholes exist in the Eurasia Basin. The closest relevant borehole is the ACEX borehole on the Lomonosov Ridge (close to the North Pole; Figs. 1B and 3) penetrating a Cenozoic succession before reaching Upper Cretaceous strata of Campanian age

(Backman *et al.* 2005, 2008; Moran *et al.* 2006a,b; Abdelmalak *et al.* 2023). A few ODP boreholes also exist on the adjacent SW Yermak Plateau (Figs. 1B and 3) providing age constraints for parts of the Neogene succession (latest Miocene and younger; Myhre *et al.* 1995; Grøsfjeld *et al.* 2014; Knies *et al.* 2014; Mattingsdal *et al*. 2014).

Boreholes on Svalbard, Franz Josef Land and in the northern Barents Sea do not provide relevant information on the Cenozoic sedimentary succession in the Eurasia Basin. Due to regional uplift and erosion of these areas (Lasabuda *et al.* 2018, 2021; Medvedev *et al.* 2022), no Cenozoic strata are preserved except for the Central Basin in Spitsbergen and the Forlandsundet Graben (Senger *et al.* 2019).

Seismic data

The seismic database in the Eurasia Basin is limited due to ice covering most of the basin throughout most of the year. Early data acquisitions were carried out from drifting ice stations (Kristoffersen *et al.* 2004; Langinen *et al.* 2009; Avetisov *et al*. 2019) and a few lines were acquired by ice breakers (e.g. Polarstern; Jokat *et al.* 1995a,b; Jokat and Micksch 2004). During recent years, an increasing amount of MCS data have been acquired by Arctic nations to support their territorial claims in the framework of the United Nations Convention on the Law of the Sea (UNCLOS) (Engen *et al.* 2009; Nikishin *et al.* 2017, 2021a; Castro *et al.* 2018). New MCS data were also acquired for planning of a second scientific drilling at the Lomonsov Ridge (Stein *et al.* 2015; Weigelt *et al.* 2020). New single channel seismic data between the Lomonosov Ridge and Morris Jesup Rise, an area inaccessible for seismic surveys by icebreakers, were acquired by using a hovercraft drifting on ice (Kristoffersen *et al.* 2021, 2022). Seismic reflection data have been complemented by seismic refraction data mainly using sonobuoys. A few OBS surveys have been carried out recently, one across the Lomonosov Ridge (Funck *et al.* 2022), one at the Gakkel Ridge (Ding *et al.* 2022), and one across the northern Svalbard/Barents Sea margin into the Nansen Basin (GoNorth 2022). Despite the new data, MCS data coverage remains poor in major parts of the Eurasia Basin (Fig. 3A).

Other data

Other relevant data comprise bathymetry and potential field (gravity and magnetic) data. The most up-to-date bathymetry grid is IBCAO 4.0 (Jakobsson *et al.* 2020). Both gravity and magnetic maps were compiled in the Circum-Arctic Mapping Project (Gaina *et al.* 2011, 2014) as part of a larger international collaborative effort also including regional geology (Harrison *et al.* 2011) and tectonic (Petrov *et al.* 2018) maps. Potential field data with focus on the Eurasia Basin are presented in Brozena *et al.* (2003) and Glebovsky *et al.* (2006).

Tectonic setting, TSE boundaries, and main tectonic /erosional/ depositional phases

Tectonic setting and boundaries

The Eurasia Basin was formed by seafloor spreading since breakup between the Barents-Kara Shelf and Lomonosov Ridge some 54-56 million years ago. Prior to that, the area experienced (extensional) tectonics leading up to breakup (Fig. 2). The basin portraits a set of well-defined magnetic anomalies resulting from the seafloor spreading (Karasik 1973; Brozena *et al*. 2003). The oldest identified magnetic chron along the basin's flanks is C24n (Savostin *et al*. 1984; Glebovsky *et al*. 2006), which, according to Walker and Geissman (2022), corresponds to ~53 Ma (earliest Eocene).

Between chron C24n and the foot of the slope on both Barents Sea and Lomonosov Ridge conjugate margins, there is an up to 100 km wide area of hyper-extended continental crust and possibly exhumed upper mantle (Jokat *et al*. 1995b; Lutz *et al*. 2018; Funck *et al*. 2022; Abdelmalak *et al*. 2023). This zone is inferred to be formed during the initial rifting and is included into the Eurasian Arctic Rifted Margin and Lomonosov Ridge CTSEs correspondingly (Abdelmalak *et al*. 2023 and 2024). Minakov *et al*. (2012; 2013) based on gravity modeling suggested a short-lived phase of shear (at ~68-56 Ma) that localized deformation before the magma-poor continental breakup in the Eurasia Basin and separation of the Lomonosov Ridge microcontinent from the Barents/Kara shelves by seafloor spreading. Based on interpretation of MCS data, Lutz *et al*. (2018) suggested that mantle exhumation was involved in the initial opening and that the Eurasia Basin basement predominantly formed by exhumed and serpentinized mantle, with magmatic additions (Fig. 5).

Based on integrated analysis of seismic reflection and refraction data across the Lomonosov Ridge and into the Eurasia Basin, Funck *et al*. (2022) presented a model for the continent-ocean transition zone (COT) comprising three distinct crustal domains (Fig. 5): (1) thin continental crust down-faulted from the main Lomonosov Ridge; (2) exhumed and serpentinized mantle with some gabbroic intrusions; and (3) oceanic crust. The possible magnetic chron C25 suggested by Brozena *et al*. (2003) is located within the inner zone of faulted thin continental crust in the Funck *et al*. (2022) model indicating that the time of breakup and onset of oceanic crust was closer to chron C24 (in the earliest Eocene).

Near the Laptev Sea, the Gakkel Ridge including its active spreading axis becomes buried beneath rather thick sedimentary accumulation known as the Lena Prodelta sourced by Siberia palaeorivers including Lena River (Sekretov 2002; Gantz *et al*. 2011). In this area, the linear magnetic anomalies

are barely detectable except for the youngest ones (Chron 6 or 5 and younger). New seismic data allow to infer some more extensive presence of the rifted continental crust beneath this basin. During RV Polarstern PS115/2 expedition in 2018 (Stein 2019b), a large amount of terrestrial siliciclastic bedrocks was dredged from slopes of a newly discovered seamount in the Amundsen Basin – some 125 km east of the spreading axis right on the projected extent of the Chron 18 (Fig. 1B). However, presently we do not have data to infer lateral extent of the discovered continental block, but its presence may suggest a more complex history of this part of the Eurasia Basin. Similar view was proposed by Shipilov *et al*. (2021).

We recognize two major sedimentary accumulations which are closely linked and partly overlapping/interfingering: (1) an oceanic basin TSE and (2) a prograded margin TSE, which when combined form the Eurasia Basin CTSE. Boundaries of both TSEs are poorly constrained. There is no clear localized boundary between them neither in the Nansen nor in the Amundsen basins due to the facies change and interfingering of prograded and aggraded hemipelagic sediments (Jokat and Micksch 2004; Engen *et al*. 2009; Lasabuda *et al*. 2018). The provisional distal boundary of the prograded TSE is guided by the thickness distribution within the huge sedimentary fans reflecting major outbuilding of sediments into the basin, mainly from the Barents-Kara and Laptev shelves (Fig. 4), as well as by the sea floor topography. Therefore, the boundary between the oceanic and prograded TSEs as shown in Fig.1B represents a rather rough approximation for a transitional zone between both TSEs.

The outer boundary of the oceanic TSE approximates onlap of the sediments onto the magmatic oceanic crust of the Gakkel Ridge (Fig. 1B). The proximal boundary of the prograded margin TSE coincides with the pinchout zone of Cenozoic strata close to the shelf edge along the Barents-Kara margin and by disappearing of clinoforms in the upper Cenozoic section on the Laptev Shelf (Fig. 1B).

In the western part of the region, we have extended the oceanic TSE towards the Fram Strait where the Gakkel Ridge transitions into the Lena Trough (Snow *et al*. 2011; Laukert *et al*. 2014; Jokat *et al*. 2016). There, the oceanic basin is narrower and bounded by the conjugate Yermak Plateau (Geissler and Jokat 2004; Jokat *et al*. 2008; Geissler *et al*. 2011; Kristoffersen *et al*. 2020) and Morris Jesup Rise (Døssing *et al*. 2014; Kristoffersen *et al*. 2021) (Fig. 1B).

Therefore, the prograded margin TSE over its entire extent rests on the rifted margins of the Eurasia Basin, overlaps the continent-ocean transition zone (COT) and onlaps onto the spreading oceanic crust while the oceanic TSE occurs in the most distal parts of the Amundsen and Nansen basins.

Main tectonic, erosional and depositional phases

Detailed studies of magnetic anomalies in the eastern Eurasia Basin suggest asymmetric spreading or ridge relocation in the Eocene from around 49 to 33 Ma (Brozena *et al*. 2003; Glebovsky *et al*. 2006; Gaina *et al*. 2015). They linked the changes of plate kinematics here to intraplate stresses originating from the northward movement (push) of Greenland that created the Eurekan deformation (Piepjohn *et al*. 2016).

The spreading rates at the Gakkel Ridge show both temporal and spatial variations. During the initial opening the rates were significantly higher than at present (Fig. 2). For the first 10 m.y. of Eocene opening Glebovsky *et al*. (2006) estimated spreading rates varying from ~28 mm/year to ~23 mm/year from west to east in the Eurasia Basin. Spreading slowed down significantly in the mid-Eocene at around 45 Ma before it became ultra-slow (according to the classification of Dick *et al*. 2003) in the earliest Oligocene. At this time, seafloor spreading terminated in the Labrador Sea-Baffin Bay system and Greenland moved together with North America in a more westerly direction (Gaina *et al*. 2009).

The Eurasia Basin is filled by large volumes of sediments prograding into the basin and mixing up with hemipelagic sediments in distal deep-water parts of the Nansen and Amundsen basins. The asymmetry between the Nansen and Amundsen basins with respect to water depth and sedimentary thickness (Fig. 4) reflects the location of the main sediment source areas. Pre-glacial sediments were mainly delivered by major river systems running across wide shelves like the Barents/Kara and Laptev Sea. Parts of the northern Barents Shelf including Svalbard were also uplifted and subjected to erosion (Blythe and Kleinspehn 1998; Dimakis *et al.* 1998; Lasabuda *et al*. 2021; Lundschien *et al*. 2023; Olaussen *et al*. 2023; Drachev *et al*. 2024b; Smelror *et al*. 2024). Another major sediment pathway has been related to the Siberian rivers, especially the Lena and Khatanga, which delivered a huge volume of sediments accumulated in the deep-water Lena Prodelta (Sekretov 2002; Grantz *et al*. 2011; Piskarev *et al*. 2018; Shipilov *et al*. 2021). Eocene sediments may also have been sourced from the uplifted Eurekan-Spitsbergen fold and thrust belt running from Ellesmere, through North Greenland to western Spitsbergen in Svalbard (Braathen *et al.* 1999; Piepjohn *et al.* 2016; Vamvaka *et al*. 2019), into the western Amundsen Basin (Castro *et al*. 2018).

By the Miocene opening of the Fram Strait gateway (Jakobsson *et al.* 2007; Engen *et al.* 2008; Jokat *et al.* 2016), ocean currents entered the Eurasia Basin giving rise to contourite deposits along the basin margins (Eiken and Hinz 1993; Geissler et al. 2011; Lasabuda *et al.* 2018; Weigelt *et al.* 2020).

Throughout the Neogene, the climate changed from greenhouse to icehouse conditions giving rise to northern hemisphere glaciations (Smith and Pickering 2003; Hutchinson *et al.* 2019; Stein 2019).

Glaciations were initiated at ~4 Ma in the northern Barents Sea/Svalbard area but the first large-scale glaciation reaching the shelf edge did not occur before ~2.75 Ma (Knies *et al.* 2014). Large volumes of glacial sediments were deposited in the Nansen Basin and Norwegian-Greenland Sea as large fans in front of the bathymetric troughs on the shelf formed by glacial erosion (e.g. Faleide *et al.* 1996; Lasabuda *et al.* 2018; Hjelstuen and Sejrup 2021).

Underlying and overlying rock assemblages

Age of underlying basement (consolidated crust), or youngest underlying sedimentary unit

The underlying basement of the CTSE seaward of the continent-ocean boundary (COB) is oceanic crystalline crust formed by seafloor spreading since the earliest Eocene. Locally within the COT, exhumed and serpentinized mantle rocks may also be present. Landward of the COB, the youngest sedimentary unit underlying the prograded margin is of Cretaceous age (Lundschien *et al.* 2023; Abdelmalak *et al.* 2024).

Age of oldest overlying sedimentary unit

The CTSE comprises Eocene to recent sediments with the present seafloor as the upper boundary.

Subdivision and internal structure

The Eurasia Basin is subdivided into two basins separated by the Gakkel Ridge representing a plate boundary (Figs. 1B and 4). The Nansen Basin, located between the Gakkel Ridge and the Barents/Kara margin, has shallower water depths and contains thicker sediments. The Amundsen Basin, located between the Gakkel Ridge and the Lomonosov Ridge, has deeper water depths and contains thinner sediments compared to the Nansen Basin (Figs. 4 and 5).

Major boundary faults of the Eurasia Basin are associated with the COB/COT along the conjugate margins of the Barents/Kara Sea and Lomonosov Ridge (Figs. 4 and 5). These are dominantly extensional in nature but may have been involved in short-lived shear during the continental breakup (Minakov *et al.* 2012, 2013; Berglar *et al.* 2016). Fault zones bounding the Yermak Plateau (Geissler and Jokat 2004; Berglar *et al.* 2016) and Morris Jesup Rise (Lincoln Sea–Klenova Valley Fault Zone; Døssing *et al.* 2014; Kristoffersen *et al.* 2021) towards the Eocene parts (chrons C24-13; Fig. 6) of the Nansen and Amundsen basins respectively, must be associated with strike-slip or oblique extension during initial opening of the Eurasia Basin. The same may be the case for the eastern

boundary of the Eurasia Basin towards the Laptev Sea margin (Khatanga-Lomonosov Transform/Fracture Zone; Drachev *et al.* 2003, 2018; Fig. 6).

The Eurasia Basin conjugate margins are likely segmented (Abdelmalak *et al*. 2023, 2024), caused by pre-existing structures oriented at a high-angle to the line of breakup (COB/COT's). The prominent bend in the Barents/Kara and Lomonosov Ridge conjugate margins, also reflected in the Gakkel Ridge, may be related to inherited structures associated with basement terrain boundaries and/or Late Paleozoic-Mesozoic rifting. However, there are no distinct offsets (transform faults) along the Gakkel Ridge (Fig. 6).

There are prominent depocentres associated with the prograded margin TSE (Fig. 7). The thickest sediment accumulation, the Lena Prodelta, is located along the Laptev Sea margin. Large sediment volumes have been shed from the Lena River, across the Laptev Sea shelf into the Eurasia Basin and even burying eastern parts of the Gakkel Ridge (Fig. 4A). Another huge depocenter is located in the Nansen Basin outside the St. Anna and Voronin troughs in the northern Barents Sea (Fig. 7).

Sedimentary fill

Total thickness

The total sedimentary thickness of the Eurasia Basin and surrounding areas is shown in Figure 7A. It is compiled from various sources (Sekretov 2002; Jokat and Micksch 2004; Døssing *et al.* 2014; Nikishin *et al.* 2021; Rekant *et al.* 2021) utilizing all available relevant data (seismic, gravity inversion, depth to magnetic basement). The Eurasia Basin fill of Eocene to present age is generally thicker in the Nansen Basin (up to 5-6 km) compared to the Amundsen Basin (1-2 km). Both basins show significant thinning and pinchout towards the Gakkel Ridge (Fig. 4; see also Nikishin *et al*. 2017).

Lithostratigraphy and seismic stratigraphy

There is no direct information on lithofacies due the lack of boreholes in the Eurasia Basin. A formal lithostratigraphy has therefore not been established in the Eurasia Basin. By correlations to IODP/ODP boreholes on the Lomonosov Ridge and Yermak Plateau (Figs. 1B and 2) we can make some inference about the age and nature/composition of the Eurasia Basin sedimentary fill.

A seismic stratigraphic framework has been proposed for various parts of the Eurasia Basin (Fig. 2 and Table 1). There are uncertainties in the correlations between the different areas/provinces due to sparse seismic data coverage and the lack of regional tie lines (Fig. 3). Age constraints are mainly

based on the age of the underlying oceanic crust, from magnetic chrons, providing a maximum age of the oldest sediments deposited above. The age of these sediments can be younger taking into account the basement topography (Fig. 4). Seismic facies analysis also contributes to the mapping of characteristic depositional units in the Eurasia Basin (e.g. Lasabuda *et al.* 2018). By analysing seismic amplitudes and geometry of reflections within each seismic unit, the depositional environment and main sedimentary process involved can be interpreted (see below).

Depositional environment and provenance

The inferred depositional environments and provenance mainly build on the seismic stratigraphic framework based on seismic facies and chronology from regional seismic correlations, combined with constraints on the uplift/erosion history of surrounding source areas (e.g. Henriksen *et al.* 2011; Sobolev 2012; Lasabuda *et al.* 2018, 2021; Zhang *et al.* 2018; Dörr *et al.* 2019a,b; Japsen *et al.* 2021a,b; 2023; Medvedev *et al.* 2022; Lundschien *et al*. 2023; Olaussen *et al*. 2023; Smelror *et al*. 2023; Drachev *et al*. 2024a,b; Drachev and Ershova 2024).

Following breakup in a hot climate at the Paleocene-Eocene transition, a narrow/elongated basin developed by initial sea floor spreading (Fig. 6C). This restricted basin had episodic fresh surface waters as manifested by the early Eocene Azolla event (~50 Ma; Brinkhuis *et al.* 2006; Speelman *et al.* 2009; Barke *et al.* 2012). Large thicknesses of lower Eocene sediments were deposited throughout most of the incipient Eurasia Basin. Castro *et al.* (2018) reported early-middle Eocene (Unit 1a; 56-45 Ma) sedimentation rates >130 m/my in the central and western Amundsen Basin, partly sourced from the Lomonosov Ridge but surrounding shelf areas may also have contributed. Weigelt *et al.* (2020) estimated sedimentation rates of >200 m/my for the same time interval (units AB-1 and AB-2) in the eastern Amundsen Basin. A thick (> 2 km) depocenter here was largely sourced from the proximal Laptev Sea shelf but other source areas may have contributed. In the western Nansen Basin, a sedimentation rate of 126 m/my has been estimated for sequence NB-1A (54-48 Ma). The reflection pattern of this sequence towards the main basin boundary fault indicates moderate depositional energy and a remote source area, and therefore a long-distance sediment routing during the early Eocene (Engen *et al.* 2009). Since ~48-45 Ma the sedimentation rates were significantly reduced both in the Nansen and Amundsen basins (Jokat *et al.* 1995a,b; Engen *et al.* 2009; Castro *et al.* 2018; Weigelt *et al.* 2020). This reduction likely reflects reduced topography and associated erosion in surrounding source areas.

Regional exhumation beginning at the end of the Eocene was widespread in the Arctic, which has been related to plate tectonic reorganizations (Green and Duddy 2010; Japsen *et al.* 2023). The uplifted areas may have contributed to mass transport deposits in parts of the Eurasia Basin. An upper Eocene-lower Oligocene sedimentary wedge in the western Amundsen Basin along the Lomonosov Ridge is interpreted as a submarine fan reflecting tectonic instability that may be related to Eurekan deformation (Castro *et al.* 2018).

The upper Oligocene – lower Miocene interval is characterized by laterally extensive parallel strata of uniform thickness. The basal onlap patterns reflect passive infill deposited in a low-energy hemipelagic setting under relative quiet tectonic conditions (Castro *et al.* 2018; Weigelt *et al.* 2020).

Sediment drifts (contourites) have accumulated along the Eurasia Basin flanks since the opening of the Fram Strait gateway in the Miocene (Lasabuda *et al.* 2018; Weigelt *et al.* 2020). An up to 1000 m thick Miocene-Pliocene sequence in the western Nansen Basin shows a mixture of marine hemipelagic and contouritic deposits. The widespread contourites deposited on the slope reflect the importance of ocean currents established from the opening of the Fram Strait gateway (Lasabuda *et al.* 2018). The widespread occurrence in the eastern Amundsen Basin of sediment waves, drifts and erosional features within unit AB-5 (20-5.3 Ma) was taken as evidence for a Miocene onset of ocean circulation and associated bottom current activity (Weigelt *et al.* 2020). The mid-upper Miocene unit 4 (17-8 Ma) in the western Amundsen Basin thickens towards the Lomonosov Ridge where it locally shows geometries reflecting depositional effects of oceanographic bottom currents (Castro *et al.* 2018).

Along the northern Barents-Kara margin, the upper Plio-Pleistocene strata form huge sedimentary fans (i.e. trough mouth fans) deposited in front of bathymetric troughs on the shelf caused by glacial erosion by ice-streams (Batchelor and Dowdeswell 2014). Glacigenic debris flows (GDF) are the main sediment type building the trough mouth fans (Laberg *et al.* 2010). The largest fans are associated with the Franz-Victoria, St. Anna and Voronin troughs (Fig. 7B). Lasabuda *et al.* (2018) estimated an average sedimentation rate of 240 m/my for the Plio-Pleistocene deposits in the western Nansen Basin derived from the northwestern Barents Sea shelf and adjacent land areas. This abrupt change in sedimentation rates reflects glacial erosion, in particular by fast-flowing ice-streams shaping the wide shelf areas and transporting large sediment volumes to the shelf break (e.g. Faleide *et al.* 1996; Andreassen *et al.* 2008; Batchelor and Dowdeswell 2014; Hjelstuen and Sejrup 2021). The thick and rapidly deposited glacial sediments are prone to slope failure, exemplified by the Hinlopen Slide on the northern Svalbard margin running into the western Nansen Basin (Vanneste *et al.* 2006; Winkelmann *et al.* 2008). Between the fans, contouritic sedimentation prevailed indicating a strong

influence of alongslope sedimentary processes (Lasabuda *et al.* 2018). A higher-energy depositional environment is also recorded in the western Amundsen Basin. Here upper Plio-Pleistocene sediments accumulated in relation to a channel system extending from the Lincoln Sea shelf margin into the Amundsen Basin (Castro *et al.* 2018). A large submarine fan is also observed in the Amundsen Basin probably sourced from the North Greenland and Canadian Arctic continental margins (Kristoffersen *et al.* 2004). Moreover, deposition of a mass transport complex adjacent to the Lomonosov Ridge is linked with the ice sheet dynamics in the region (Perez *et al.* 2020; Schlager *et al.* 2021).

8. Magmatism

The Paleogene breakup was largely magma-poor (Minakov *et al.* 2012, 2013; Lutz *et al.* 2018; Funck *et al.* 2022) before the onset of seafloor spreading in the Eurasia Basin. However, the area has been affected by younger magmatism during the Cenozoic evolution. The crustal thickness of Yermak Plateau and Morris Jesup Rise had increased by magmatic addition before they separated at the Eocene-Oligocene transition (~34 Ma). Kristoffersen *et al.* (2020) suggested an age corresponding to chron C22-18 (49-39 Ma) for this magmatism. In Svalbard, both Miocene (~10 Ma; Prestvik 1978) and Quaternary (Amundsen *et al.* 1987) magmatism are known. Dredged basalt at the flanks of the Mosby seamount in the Sophia Basin (Fig. 1B) has been dated ~13 Ma (Geissler *et al.* 2019).

9. Heat flow

Heat flow data in the Eurasia Basin are sparse and unevenly distributed (Struijk *et al*. 2018; Fuchs *et al*. 2021, 2023), and were collected mainly along the Gakkel Ridge with a few measurements in the Amundsen Basin (Urlaub and Jokat 2009; Xiao 2013; Shephard *et al*. 2018). A few data points were also acquired during the PANORAMA expedition in the SW Nansen Basin and SE Yermak Plateau (Damm *et al*. 2013) (Fig. 3B). Sundvor *et al.* (2000) reported high heat flow values (855 and 1164 mW m^{-2}) measured on the Gakkel Ridge, likely reflecting active volcanism and/or venting along the plate boundary. Urlaub *et al.* (2009) presented a series of heat flow measurements along the Gakkel Ridge having a scatter of values around 150 mWm^{-2} with extremes as high as 426 mW m^{-2}. Recent heat flow measurements in the Western Volcanic Zone of the Gakkel Ridge (Fig. 3B) are in the range 734-

1825 mW m^{-2} (Dziadek *et al.* 2021). Measurements in the Amundsen Basin vary between 71 and 127 mW m^{-2} (Urlaub *et al.* 2009; Shephard *et al.* 2018) while a few measurements in the Sophia and Nansen basins and adjacent part of the Yermak Plateau have values in the 50-80 mW m^{-2} range (Sundvor *et al.* 2000; Damm *et al.* 2013). Heat flow measurements in the Kvitøya Trough NE of Svalbard (Fig. 3B) gave surprisingly high values of 340 mW m^{-2} (Zayonchek *et al.* 2009), which may be related to the recent magmatism known in northern Spitsbergen. Heat advection by fluids may also have affected these high readings. Heat flow measurements from the Laptev Sea margin have values around 100 mW m^{-2} (Drachev *et al.* 2003).

10. Petroleum geology

Discovered and potential petroleum resources

Due to complete lack of boreholes, no hydrocarbon accumulations have been discovered. Given the oceanic nature of the Eurasia Basin, the hydrocarbon potential is likely low. However, some potential may still exist in relation to the systems briefly described below.

Current exploration status

Most of the Eurasia Basin is ice-covered most of the year. This fact, combined with the vulnerable environment, explain why the area has not been open for petroleum exploration. Geopolitical issues, such as overlapping claims with respect to the outer limits of the continental shelf of the Arctic coastal states have also contributed to this.

Hydrocarbon systems and plays

For the same reasons described above, no proven hydrocarbon systems exist. However, there are indications of working petroleum system(s) (Moore and Pitman 2011). Blumenberg *et al.* (2016) analysed near-surface sediments at the northern Barents Sea (Hinlopen) margin and adjacent parts of the Nansen Basin, and found possible indications of subsurface hydrocarbon generation. Sokolov *et al*. (2023) reported seismic amplitude anomalies in the Cenozoic sediments of the Nansen Basin indicating gas generation (Fig. 3B).

Source rocks. A potential source rock exists in the lower-middle Eocene strata, in particular the Azolla interval (~50 Ma) characterized by abundant freshwater algae fossils widely distributed in the Arctic (Brinkhuis *et al.* 2006; Whaley 2007; Speelman *et al.* 2009; Barke *et al.* 2012). At the

Lomonosov Ridge, it was penetrated by the ACEX borehole having TOC values exceeding 5%. Here, it is immature due to limited overburden but in adjacent basins it may be buried deep enough for hydrocarbon generation (Mann *et al.* 2009). In the Eurasia Basin, we should expect to find Azolla in parts of the basin being older than chron C21, in the Nansen and Amundsen basins respectively. Here Azolla was deposited in an enclosed narrow/elongated basin with restricted bottom water circulation causing anoxic conditions. In some areas the lower-middle Eocene potential source rock is too deeply buried. In parts of the Lena Prodelta where this source rock is present, along both conjugate margins off the Lomonosov Ridge and Taimyr, it is buried to depths >6 km (Figs. 4A and 7A). Moore and Pitman (2011) analysed a pseudo well in such a position and concluded that the lower-middle Eocene source rock is overmature. More optimal burial of this source rock could be in the depocenters of the trough mouth fans along the northern Barents-Kara Sea margin (Franz Victoria Fan, St. Anna Fan, Voronin Fan; Figs. 1A and 7B). Blumenberg *et al.* (2016) modeled the thermal and maturation history for a pseudo well located in the SW Nansen Basin and their simulations indicate that a tentative Azolla source rock entered the early oil window in early Miocene time. The Lena Prodelta may contain younger source rocks deposited within the prograding delta system and these could eventually lie in the oil window (Moore and Pitman 2011). Below the prograded and rifted margins in the northern Barents Sea, older Mesozoic source rocks (Middle Triassic, Upper Jurassic) may be present (Lundschien *et al.* 2021).

Reservoirs. Mesozoic (Upper Triassic-Lower/Middle Jurassic) coarse siliciclastic rocks were eroded on the NW Barents Shelf during the Cenozoic uplift and erosion (Lasabuda *et al*. 2021) providing siliciclastic material for potential Cenozoic reservoirs in the western Nansen Basin. Other areas may also have potential for clastic reservoir units, particularly gravity-driven deposits of sandy turbidite channels within submarine fans (Castro *et al*. 2018). Reservoir rocks are not proven in the Lena Prodelta but lithic-rich siliciclastics may have reached deepwater parts of the Lena delta systems (Moore and Pitman 2011).

Seals. The main sealing potential is expected to be associated with fine-grained contourites and glacigenic debrites. In particular, the thick shale-rich trough mouth fans may form a regional seal in some parts of the Eurasia Basin. The present subcrop geology on the Barents Shelf is dominated by Lower Cretaceous shales – erosional products of these should be fine-grained clayey sediments having sealing capacities. If reservoir rocks are present in the Lena Prodelta they should be encased in hemipelagic mudstone providing good sealing (Moore and Pitman 2011).

Traps. Based on the depositional setting we expect to find mainly stratigraphic traps within the Eurasia Basin CTSE. For example, the sandy part of submarine fans may be trapped in between finer-

grained sediments of contourites or mass-transport deposits. They may also be pinched out stratigraphically in the proximal part where hydrocarbon accumulations would be trapped upslope the northern Barents Shelf or in the adjacent structural highs.

Acknowledgements

We acknowledge the support from the Research Council of Norway through the DYPOLE project 325984. Finally, we thank the volume editors and the reviewers Wilfried Jokat and Ruth Jackson.

References

Abdelmalak, M.M., Minakov, A., Faleide, J.I. and Drachev, S.S. 2023. The Lomonosov Ridge Composite Tectono-Sedimentary Element. *Geological Society, London, Memoirs*, **57**,

Abdelmalak, M.M., Meza Cala, J.C., Minakov, A., *et al*. 2024. Eurasian Arctic Rifted Margin Composite Tectono-Sedimentary Element. *Geological Society, London, Memoirs*, **57**,

Amundsen, H.E.F., Griffin, W.L. and O'Reilly, S.Y. 1987. The lower crust and upper mantle beneath northwestern Spitsbergen: evidence from xenoliths and geophysics. *Tectonophysics*, **139**, 169-185.

Andreassen, K., Laberg, J.S. and Vorren, T.O. 2008. Seafloor geomorphology of the SW Barents Sea and its glaci-dynamic implications. *Geomorphology*, **97**, 157–177. https://doi.org/10.1016/j.geomorph.2007.02.050

Avetisov, G.P., Butsenko, V.V. et al. 2019. The Current State of the Arctic Basin Study. In: Piskarev, A., Poselov, V. and Kaminsky, V. (eds.), Geologic Structures of the Arctic Basin. Cham, Springer International Publishing, p. 1-70.

Backman, J., Moran, K., McInroy, D., and the, I. E. S. 2005. IODP Expedition 302, Arctic Coring Expedition (ACEX): A First Look at the Cenozoic Paleoceanography of the Central Arctic Ocean: Sci. Dril., v. 1, p. 12-17.

Backman, J., Jakobsson, M., Frank, M., *et al*. 2008. Age model and core-seismic integration for the Cenozoic Arctic Coring Expedition sediments from the Lomonosov Ridge. *Paleoceanography*, **23**, no. 1.

Barke, J., van der Burgh, J., van Konijnenburg-van Cittert, J.H.A., *et al*. 2012. Coeval Eocene blooms of the freshwater fern Azolla in and around Arctic and Nordic seas. *Palaeogeography, Palaeoclimatology, Palaeoecology*, **337–338**, 108–119, doi:10.1016/j.palaeo.2012.04.002

Batchelor, C. and Dowdeswell, J. 2014. The physiography of High Arctic cross-shelf troughs. *Quaternary Science Reviews*, **92**, 68–96. https://doi.org/10.1016/j.quascirev.2013.05.025

Berglar, K., Franke, D., Lutz, R., Schreckenberger, B. and Damm, V. 2016. Initial opening of the Eurasian Basin, Arctic Ocean. *Frontiers in Earth Science*, **4**, 91. https://doi.org/10.3389/feart.2016.00091

Blumenberg, M., Lutz, R., Schlömer, S., *et al*. 2016. Hydrocarbons from near-surface sediments of the Barents Sea north of Svalbard - Indication of subsurface hydrocarbon generation? *Marine and Petroleum Geology*, **76**, 432-443. http://dx.doi.org/10.1016/j.marpetgeo.2016.05.031

Blythe, A.E. and Kleinspehn, K.L. 1998. Tectonically versus climatically driven Cenozoic exhumation of the Eurasian plate margin, Svalbard: Fission track analyses. *Tectonics*, **17**, 621-639.

Brinkhuis, H., Schouten, S., Collinson, M. E., *et al*. 2006. Episodic fresh surface waters in the Eocene Arctic Ocean. *Nature*, **441**, 7093, 606-609.

Brotzer, A., Funck, T., Geissler, W.H., *et al*. 2022, Geophysical insights on the crustal structure of Greenland's northern continental margin towards the Morris Jesup Spur: Tectonophysics, v. 843, p. 229588.

Brozena, J., Childers, V., Lawver, L., Gahagan, L., Forsberg, R., Faleide, J. and Eldholm, O. 2003. New aerogeophysical study of the Eurasia Basin and Lomonosov Ridge: Implications for basin development: *Geology*, **31**, 825-828.

Braathen, A., Bergh, S.G. and Maher, H.D., Jr. 1999. Application of a critical wedge taper model to the Tertiary transpressional fold–thrust belt on Spitsbergen. *Geological Society of America Bulletin*, **111**, 1468–1485.

Cai, Y., Yang, A.Y., Goldstein, S.L., *et al*. 2021. Multi-stage melting of enriched mantle components along the eastern Gakkel Ridge. *Chemical Geology*, **586**, 120594.

Castro, C. F., Knutz, P. C., Hopper, J. R. and Funck, T. 2018. Depositional evolution of the western Amundsen Basin, Arctic Ocean: paleoceanographic and tectonic implications. *Paleoceanography and Paleoclimatology*, **33**, 1357-1382.

Chernykh, A.A. and Krylov, A.A. 2011. Sedimentogenesis in the Amundsen Basin from geophysical data and drilling results on the Lomonosov Ridge. *Doklady Earth Sciences*, **440**, 1372-1376.

Chernykh, A.A. and Krylov, A.A. 2017. Duration, causes, and geodynamic significance of the Middle Cenozoic Hiatus in sedimentation in the near-polar part of the LR (based on IODP-302-ACEX drilling data). *Oceanology*, **57**, 675–684. https://doi.org/10.1134/S0001437017050058

Cochran, J.R., Kurras, G.J., Edwards, M.H. and Coakley, B.J. 2003. The Gakkel Ridge: Bathymetry, gravity anomalies, and crustal accretion at extremely slow spreading rates. *J. Geophys. Res.*, **108**, 2116, doi:10.1029/2002JB001830, 2003.

Damm, V., et al. 2013. Cruise Report BGR13-2, Project: PANORAMA-1.

http://www.bgr.bund.de/DE/Themen/MarineRohstofforschung/Meeresforschung/Projekte/NIL/Berichte_Expedition_Panorama1.htm

Dick, H., Lin, J. and Schouten, H. 2003. An ultraslow-spreading class of ocean ridge. *Nature*, **426**, 405-412.

Dimakis, P., Braathen, B.I., Faleide, J.I., Elverhøi, A. and Gudlaugsson, S.T. 1998. Cenozoic erosion and the preglacial uplift of the Svalbard–Barents Sea region. *Tectonophysics*, **300**, 311-327.

Ding, W., Niu, X., Zhang, T., et al. 2022. Submarine wide-angle seismic experiments in the High Arctic: The JASMInE Expedition in the slowest spreading Gakkel Ridge. *Geosystems and Geoenvironment*, **1**, 100076.

Drachev, S.S. and Shkarubo, S.I. 2018. Tectonics of the Laptev Shelf, Siberian Arctic. *Geological Society, London, Special Publications*, **460**, 263–283.

Drachev, S.S. and Ershova, V. 2024. North Kara and Vize-Ushakov Composite Tectono-Sedimentary Elements, Kara Sea. Geological Society, London, Memoirs, 57, 1155 https://doi.org/10.1144/M57-???

Drachev, S.S., Kaul, N. and Beliaev, V.N. 2003. Eurasia spreading basin to Laptev Shelf transition: structural pattern and heat flow. *Geophysical Journal International*, **152**, 688–698.

Drachev, S.S., Mazur, S., Campbell, S., *et al*. 2018. Crustal architecture of the Laptev Rift System in the East Siberian Arctic based on 2D long-offset seismic profiles and gravity modelling. *Petroleum Geoscience*, **24**, 402-413. https://doi.org/10.1144/petgeo2016-143.

Drachev, S.S., Ershova, V. and Shkarubo, S.I. 2024a. Laptev Rift System Composite Tectono-Sedimentary Element, East Siberian Arctic. Geological Society, London, Memoirs, 57, 1155 https://doi.org/10.1144/M57-???

Drachev, S.S., Henriksen, E., Shkarubo, S.I. and Sobolev, P. 2024b. East Barents and Admiralty High Composite Tectono-Sedimentary Elements, Barents Sea. Geological Society, London, Memoirs, 57, https://doi.org/10.1144/M57-2021-39

Dziadek, R., Doll, M., Warnke, F. and Schlindwein, V. 2021. Towards Closing the Polar Gap: New Marine

Heat Flow Observations in Antarctica and the Arctic Ocean. *Geosciences*, **11**, 11.

https://dx.doi.org/10.3390/geosciences11010011

Døssing, A., Hopper, J.R., Olesen, A.V., Rasmussen, T.M. and Halpenny, J. 2013. New aerogravity results from the Arctic Ocean: Linking the latest Cretaceous-early Cenozoic plate kinematics of the North Atlantic and Arctic Ocean. *Geochem Geophys Geosyst*, **14**, 4044-4065.

Døssing, A., Hansen, T.M., Olesen, A.V., Hopper, J.R. and Funck, T. 2014. Gravity inversion predicts the nature of the Amundsen Basin and its continental borderlands near Greenland. *Earth and Planetary Science Letters*, **408**, 132-145.

Eiken, O. and Hinz, K. 1993. Contourites in the Fram Strait. *Sedimentary Geology*, **82**, 15–32. https://doi.org/10.1016/0037-0738(93)90110-Q

Engen, Ø., Eldholm, O. and Bungum, H. 2003. The Arctic plate boundary. *J. Geophys. Res.*, **108** http://dx.doi.org/10.1029/2002jb001809.

Engen, Ø., Faleide, J.I. and Dyreng, T.K. 2008. Opening of the Fram Strait gateway: A review of plate tectonic constraints. *Tectonophysics*, **450**, 51-69.

Engen, Ø., Gjengedal, J.A., Faleide, J.I., Kristoffersen, Y. and & Eldholm, O. 2009. Seismic stratigraphy and sediment thickness of the Nansen Basin, Arctic Ocean. *Geophysical Journal International*, **176**, 805–821. https://doi.org/10.1111/j.1365-246X.2008.04028.x

Faleide, J.I., Solheim, A., Fiedler, A., Hjelstuen, B.O., Andersen, E.S. and Vanneste, K. 1996. Late Cenozoic evolution of the western Barents Sea-Svalbard continental margin. *Global and Planetary Change*, **12**, 53-74.

Fuchs, S., Beardsmore, G., Chiozzi, P., *et al*. 2021. A new database structure for the IHFC Global Heat Flow Database. *International Journal of Terrestrial Heat Flow and Applied Geothermics*, **4**, 14 p. doi:https://doi.org/10.31214/ijthfa.v4i1.62

Fuchs, S., Norden, B., Florian Neumann, F., *et al*. 2023. Quality-assurance of heat-flow data: The new structure and evaluation scheme of the IHFC Global Heat Flow Database. *Tectonophysics*, **863**, 229976. https://doi.org/10.1016/j.tecto.2023.229976

Funck, T., Shimeld, J. and Salisbury, M.H. 2022. Magmatic and rifting-related features of the Lomonosov Ridge, and relationships to the continent–ocean transition zone in the Amundsen Basin, Arctic Ocean. *Geophysical Journal International*, **229**, 1309-1337.

Funck, T. and Shimeld, J. 2023, Crustal structure and magmatism of the Marvin Spur and northern Alpha Ridge, Arctic Ocean: Geophysical Journal International, v. 233, no. 1, p. 740-768.

Gaina, C., Gernigon, L. and Ball, P. 2009. Palaeocene–Recent plate boundaries in the NE Atlantic and the formation of the Jan Mayen microcontinent. *Journal of the Geological Society, London*, **166**, 601–616.

doi: 10.1144/0016-76492008-112.

Gaina, C., Werner, S. C., Saltus, R., Maus, S. and the CAMP-GM GROUP 2011. Chapter 3 Circum-Arctic mapping project: new magnetic and gravity anomaly maps of the Arctic. *Geological Society, London, Memoirs*, **35**, 39-48.

Gaina, C., Medvedev, S., Torsvik, T.H., Koulakov, I. and Werner, S.C. 2014. 4D Arctic: a glimpse into the structure and evolution of the Arctic in the light of new geophysical maps, plate tectonics and tomographic models. *Surv. Geophys.*, **35**, 1095-1122. http://dx.doi.org/10.1007/s10712-013-9254-y.

Gaina, C., Nikishin, A.M. and Petrov, E.I. 2015. Ultraslow spreading, ridge relocation and compressional events in the East Arctic region – A link to the Eurekan orogeny? *Arktos*, **1**, 1-11. DOI 10.1007/s41063-015-0006-8

Geissler, W.H. and Jokat, W. 2004. A geophysical study of the northern Svalbard continental margin. *Geophysical Journal International*, **6**, 50–66. https://doi.org/10.1038/srep38529

Geissler, W., Jokat, W. and Brekke, H. 2011. The Yermak Plateau in the Arctic Ocean in the light of reflection seismic data—Implication for its tectonic and sedimentary evolution. *Geophysical Journal International*, **187**, 1334–1362. https://doi.org/10.1111/j.1365-246X.2011.05197.x

Geissler, W. H., Estrada, S., Riefstahl, F., O'Connor, J. M., Spiegel, C., Van den Boogard, P. and Klügel, A. 2019. Middle Miocene magmatic activity in the Sophia Basin, Arctic Ocean—evidence from dredged basalt at the flanks of Mosby Seamount. *Arktos*, **5**, 31-48.

Glebovsky, V.Y., Kaminsky, V.D., Minakov, A.N., Merkur'ev, S.A., Childers, V.A. and Brozena, J.M. 2006. Formation of the Eurasia Basin in the Arctic Ocean as inferred from geohistorical analysis of the anomalous magnetic field. *Geotectonics*, **40**, 263-281.

Global Heat Flow Compilation, G., 2013, Component parts of the World Heat Flow Data Collection, PANGAEA.

GoNorth 2022. Laberg, J.S. (Editor) Cruise report, GoNorth-2022.

Grantz, A., Pease, V.L., Willard, D.A., *et al*. 2001. Bedrock cores from 89° North: Implications for the geologic framework and Neogene paleoceanography of Lomonosov Ridge and a tie to the Barents shelf: *GSA Bulletin*, **113**, 1272-1281.

Grantz, A., Scott, R.A., Drachev, S.S., Moore, T.E. and Valin, Z.C. 2011. Sedimentary successions of the Arctic Region (58–64° to90°N) that may be prospective for hydrocarbons. Geological Society, London, Memoirs, 35, 17–37, https://doi.org/10.1144/M35.2

Green, P. and Duddy, I. 2010. Synchronous exhumation events around the Arctic including examples from Barents Sea and Alaska North Slope. *Geological Society of London, Petroleum Geology Conference series*, **7**, 633–644. https://doi.org/10.1144/0070633

Grøsfjeld, K., De Schepper, S., Fabian, K., Husum, K., Baranwal, S., Andreassen, K. and Knies, J. 2014. Dating and palaeoenvironmental reconstruction of the sediments around the Miocene/Pliocene boundary in Yermak Plateau ODP Hole 911A using marine palynology. *Palaeogeography, Palaeoclimatology, Palaeoecology*, **414**, 382-402.

Hjelstuen, B.O. and Sejrup, H.P. 2021. Latitudinal variability in the Quaternary development of the Eurasian ice sheets - Evidence from the marine domain. *Geology*, **49**, 346-351.

Hutchinson et al. (2019) Arctic closure as a trigger for Atlantic overturning at the Eocene-Oligocene Transition. *Nature Commun*, **10**, 3797

Jackson, H.R., Dahl-Jensen, T., *et al*. 2010, Sedimentary and crustal structure from the Ellesmere Island and Greenland continental shelves onto the Lomonosov Ridge, Arctic Ocean: *Geophysical Journal International*, **182**, 11-35.

Jakobsson, M., Backman, J., Rudels, B., et al. 2007. The early Miocene onset of a ventilated circulation regime in the Arctic Ocean. *Nature*, **447**, 986-990.

Jakobsson, M., Mayer, L. A., *et al*. 2020, The International Bathymetric Chart of the Arctic Ocean Version 4.0. *Scientific Data*, **7**, 1, 176.

Jokat, W. and Micksch, U. 2004. Sedimentary structure of the Nansen and Amundsen basins, Arctic Ocean. *Geophysical Research Letters*, **31**, L02603. https://doi.org/10.1029/2003GL018352

Jokat, W., Weigelt, E., Kristoffersen, Y., Rasmussen, T. and Schöone, T. 1995a. New geophysical results from the south-western Eurasian Basin (Morris Jesup Rise, Gakkel Ridge, Yermak Plateau) and the Fram Strait. *Geophys. J. Int.*, **123**, 601-610

Jokat, W., Weigelt, E., Kristoffersen, Y., Rasmussen, T. and Schöone, T. 1995b. New insights into the evolution of the Lomonosov Ridge and the Eurasian Basin. *Geophysical Journal International*, **122**, 378-392.

Jokat, W., Ritzmann, O., Schmidt-Aursch, M.C., Drachev, S., Gauger, S. and Snow, J. 2003. Geophysical evidence for reduced melt production on the Arctic ultraslow Gakkel mid-ocean ridge. *Nature*, **423**, 962-965.

Jokat, W., Geissler, W. and Voss, M. 2008. Basement structure of the north-western Yermak Plateau. *Geophysical Research Letters*, **35**, L05309. https://doi.org/10.1029/2007GL032892

Jokat, W., Ickrath, M. and O'Connor, J. 2013. Seismic transect across the Lomonosov and Mendeleev Ridges:

Constraints on the geological evolution of the Amerasia Basin, Arctic Ocean. Geophysical Research Letter, **40**, 5047-5051.

Jokat, W., Lehmann, P., Damaske, D. and Nelson, J.B. 2016. Magnetic signature of North-East Greenland, the Morris Jesup Rise, the Yermak Plateau, the central Fram Strait: Constraints for the rift/drift history between Greenland and Svalbard since the Eocene. *Tectonophysics*, **691**, 98–109. https://doi.org/10.1016/j.tecto.2015.12.002

Jokat, W., O'Connor, J., Hauff, F., Koppers, A.A.P. and Miggins, D.P. 2019. Ultraslow spreading and

volcanism at the eastern end of Gakkel Ridge, Arctic Ocean. *Geochemistry, Geophysics, Geosystems*, **20**,

https://doi.org/10.1029/2019GC008297

Karasik, A.M. 1973. Anomalous magnetic field of Eurasian Basin of the Arctic Sea. Dokl. Akad. Nauk. SSSR, 211: No. 1 (in Russian).

Knies, J., Matthiessen, J., Vogt, C., Laberg, J. S., Hjelstuen, B. O., Smelror, M., et al. 2009. The Plio-Pleistocene glaciation of the Barents Sea–Svalbard region: A new model based on revised chronostratigraphy. *Quaternary Science Reviews*, **28**, 812–829. https://doi.org/10.1016/j.quascirev.2008.12.002

Knies, J., Mattingsdal, R., Fabian, K., Grøsfjeld, K., Baranwal, S., Husum, K., et al. 2014. Effect of early Pliocene uplift on late Pliocene cooling in the Arctic–Atlantic gateway. *Earth and Planetary Science Letters*, **387**, 132–144. https://doi.org/10.1016/j.epsl.2013.11.007

Knudsen, C., Hopper, J.R., Bierman, P.R., *et al*. 2018, Samples from the Lomonosov Ridge place new constraints on the geological evolution of the Arctic Ocean: Geological Society, London, Special Publications, 460, 397.

Kristoffersen, Y., Grantz, A., Johnson, L. and Sweeney, J.F. 1990. Eurasia Basin. *The Geology of North America*, **50**, 365–378.

Kristoffersen, Y., Sorokin, M. Y., Jokat, W. and Svendsen, O. 2004. A submarine fan in the Amundsen Basin, Arctic Ocean. *Marine Geology*, **204**, 317–324. https://doi.org/10.1016/S0025-3227(03)00373-6

Kristoffersen, Y., Ohta, Y. and Hall, J.K. 2020. On the the origin of the Yermak Plateau in the Arctic Ocean north of Svalbard. *Norwegian Journal of Geology*, **100**, 202006, https://dx.doi.org/10.17850/njg100-1-5.

Kristoffersen, Y., Hall, J.K. and Harris Nilsen, E. 2021. Morris Jesup Spur and -Rise north of Greenland – exploring present seabed features, the history of sediment deposition, volcanism and tectonic deformation at a Late Cretaceous/early Cenozoic triple junction in the Arctic Ocean. *Norwegian Journal of Geology*, **101**, 202104. https://doi.org/10.17850/njg101-1-4.

Kristoffersen, Y., Hall, J.K. and Nilsen, E.H. 2022. Sediment deformation atop the Lomonosov Ridge, central Arctic Ocean: Evidence for gas-charged sediment mobilization? *Marine and Petroleum Geology*, **138**, 105555.

Laberg, J.S., Andreassen, K., Knies, J., Vorren, T.O. and Winsborrow, M. 2010. Late Pliocene–Pleistocene development of the Barents Sea ice sheet. *Geology*, **38**, 107–110. https://doi.org/10.1130/G30193.1

Langinen, A.E., Lebedeva-Ivanova, N.N., Gee, D.G. and Zamansky, Y.Y. 2009. Correlations between the Lomonosov Ridge, Marvin Spur and adjacent basins of the Arctic Ocean based on seismic data. *Tectonophysics*, **472**, 309-322.

Lasabuda, A., Geissler, W. H., Laberg, J. S., Knutsen, S. M., Rydningen, T. A. and Berglar, K. 2018. Late Cenozoic erosion estimates for the northern Barents Sea: Quantifying glacial sediment input to the Arctic Ocean. *Geochemistry, Geophysics, Geosystems,* **19**, 4876-4903.

Lasabuda, A.P., Johansen, N.S., Laberg, J.S., Faleide, J.I., *et al.* 2021 Cenozoic uplift and erosion of the Norwegian Barents Shelf–a review. *Earth-Science Reviews*, **217**, 103609.

Laukert, G., von der Handt, A., Hellebrand, E., *et al.* 2014. High-pressure Reactive Melt Stagnation

Recorded in Abyssal Pyroxenites from the Ultraslow-spreading LenaTrough, Arctic Ocean. *Journal of Petrology*, **55**, 427-458.

Lucazeau, F. 2019, Analysis and Mapping of an Updated Terrestrial Heat Flow Data Set. *Geochemistry, Geophysics, Geosystems,* **20**, 4001-4024.

Lundschien, B.A., Mattingsdal, R., Johansen, S.K. and Knutsen, S.-M. 2023. North Barents Composite Tectono-Sedimentary Element. Geological Society, London, Memoirs, 57, https://doi.org/10.1144/M57-2021-39

Lutz, R., Franke, D., Berglar, K., Heyde, I., Schreckenberger, B., Klitzke, P. and Geissler, W.H. 2018. Evidence for mantle exhumation since the early evolution of the slow-spreading Gakkel Ridge, Arctic Ocean. *Journal of Geodynamics*, **118**, 154-165.

Mann, U., Knies, J., Chand, S., Jokat, W., Stein, R. and Zweigel, J. 2009. Evaluation and modelling of Tertiary source rocks in the central Arctic Ocean. *Marine and Petroleum Geology*, **26**, 1624-1639.

Mattingsdal, R., Knies, J., Andreassen, K., Fabian, K., Husum, K., Grøsfjeld, K. and De Schepper, S. 2014. A new 6 Myr stratigraphic framework for the Atlantic–Arctic gateway. *Quaternary Science Reviews*, **92**, 170–178. https://doi.org/10.1016/j.quascirev.2013.08.022

Mau, S., Römer, M. *et al.* 2017. Widespread methane seepage along the continental margin off Svalbard – from Bjørnøya to Kongsfjorden. Nature Scientific Reports, 7, 42997, https://doi.org/10.1038/srep42997

Medvedev, S., Faleide, J.I. and Hartz, E. 2022. Cenozoic reshaping of the Barents-Kara Shelf: Influence of erosion, sedimentation, and glaciation. *Geomorphology*, **420**, 108500

Michael, P.J., Langmuir, C.H., Dick, H.J.B., *et al.* 2003. Magmatic and amagmatic seafloor generation at the ultraslow-spreading Gakkel ridge, Arctic Ocean. *Nature*, **423** (6943), 956-961.

Minakov, A., Faleide, J. I., Glebovsky, V. Y. and Mjelde, R. 2012. Structure and evolution of the northern Barents-Kara Sea continental margin from integrated analysis of potential fields, bathymetry and sparse seismic data. *Geophysical Journal International*, **188**, 79-102.

Minakov, A.N., Podladchikov, Y.Y., Faleide, J.I. and Huismans, R.S. 2013. Rifting assisted by shear heating and formation of the Lomonosov Ridge. *Earth and Planetary Science Letters*, **373**, 31-40.

Moore, T.E. and Pitman, J.K. 2011. Chapter 48 Geology and petroleum potential of the Eurasia Basin.

Geological Society, London, Memoirs, **35**, 731–750, DOI: 10.1144/M35.48

Moran, K., Backman, J., *et al*. 2006. The Cenozoic palaeoenvironment of the Arctic Ocean. *Nature*, **441**, 7093, 601-605.

Moran, K., *et al*. 2006. The Arctic Coring Expedition (ACEX) Recovers a Cenozoic History of the Arctic

Ocean. *Oceanography*, DOI: 10.5670/oceanog.2006.14

Myhre, A., Thiede, J. and Firth, J.A., 1995. Proceedings of the Ocean Drilling Program, Initial Reports 151. Ocean Drilling Program, College Station, Texas, USA (951 pp.).

Nikishin, A., Petrov, E., Malyshev, N. and Ershova, V. 2017. Rift systems of the Russian Eastern Arctic shelf and Arctic deep water basins: link between geological history and geodynamics. *Geodynamics & Tectonophysics*, **8**, 11-43.

Nikishin, A.M., Gaina, C., Petrov, E.I., Malyshev, N.A. and Freiman, S.I. 2018. Eurasia Basin and Gakkel Ridge, Arctic Ocean: Crustal asymmetry, ultraslow spreading and continental rifting revealed by new seismic data. *Tectonophysics*, **746**, 64–82, https://doi.org/10.1016/j.tecto.2017.09.006

Nikishin, A.M., Petrov, E.I., Cloetingh, S., *et al*. 2021a. Arctic Ocean Mega Project: Paper 1 - Data collection. *Earth-Science Reviews*, **217**, 103559.

Nikishin, A.M., Petrov, E.I., Cloetingh, S., et al. 2021b. Arctic Ocean Mega Project: Paper 2 – Arctic stratigraphy and regional tectonic structure. *Earth-Science Reviews*, **217**, 103581.

Olaussen, S., Grundvåg, S.-A. et al. 2023. Svalbard Composite Tectono-Sedimentary Element, Barents Sea. Geological Society, London, Memoirs, 57, https://doi.org/10.1144/ M57-2021-36

O'Regan, M. 2011, Late Cenozoic Paleoceanography of the Central Arctic Ocean: IOP Conference Series: Earth and Environmental Science, 14, 012002.

Pérez, L.F., Jakobsson, M., Funck, T., *et al*. 2020. Late Quaternary sedimentary processes in the central Arctic Ocean inferred from geophysical mapping. *Geomorphology*, **369**, 107309. https://doi.org/10.1016/j.geomorph.2020.107309

Piepjohn, K., von Gosen, W. and Tessensohn, F. 2016. The Eurekan deformation in theArctic: an outline. *Journal of the Geological Society, London*, **173**, 1007–1024, https://doi.org/10.1144/jgs2016-081

Piskarev, A.L., Avetisov, G.P., Kireev, A.A., *et al*. 2018. Structure of the Laptev Sea Shelf–Eurasian Basin Transition Zone (Arctic Ocean). *Geotectonics*, **52**, 589–608.

Piskarev, A.L., Butsenko, V.V., Chernykh, A.A., et al. 2019. Lomonosov Ridge, in Piskarev, A., Poselov, V., and Kaminsky, V., eds., Geologic Structures of the Arctic Basin: Cham, Springer International Publishing, p. 157-185.

Poselov, V.A., Avetisov, G.P., Butsenko, V.V., *et al*. 2012. The Lomonosov Ridge as a natural extension of the Eurasian continental margin into the Arctic Basin. *Russian Geology and Geophysics*, **53**, 1276-1290.

Prestvik, T. 1978. Cenozoic Plateau Lavas of Spitsbergen: a Geochemical Study. Norsk Polarinst Årbok

Rekant, P., Sobolev, N., Portnov, A., *et al*. 2019. Basement segmentation and tectonic structure of the Lomonosov Ridge, arctic Ocean: Insights from bedrock geochronology. *Journal of Geodynamics*, **128**, 38-54.

Rekant, P.V., Petrov, O.V. and Gusev, E.A. 2021. Model of Formation of the Sedimentary System of the Eurasian Basin, the Arctic Ocean, as a Basis for Reconstructing Its Tectonic Evolution. *Geotectonics*, **55**, 676-696.

Savostin, L.A., Karasik, A.M. and Zonenshain, L.P. 1984. The history of the opening of the Eurasia basin in the Arctic. Trans. USSR Acad. Sci. 275, 79–83.

Schlager, U., Jokat, W., Weigelt, E. and Gebhardt, C. 2021. Submarine landslides along the Siberian termination of the Lomonosov Ridge, Arctic Ocean. Geomorphology, **382**, 107679.

Sekretov, S.B. (2002). Structure and tectonic evolution of the Southern Eurasia Basin, Arctic Ocean. *Tectonophysics*, **351**, 193–243.

Senger, K., Brugmans, P., Grundvåg, S.-A., Jochmann, M., Nøttvedt, A., Olaussen, S., Skotte, A. and Smyrak-Sikora, A. 2019. Petroleum, coal and research drilling onshore Svalbard: a historical perspective. *Norwegian Journal of Geology*, **99**. https://dx.doi.org/10.17850/njg99-3-1.

Shephard, G.E., Wiers, S., Bazhenova, E., et al. 2018. A North Pole thermal anomaly? Evidence from new and existing heat flow measurements from the central Arctic Ocean. *Journal of Geodynamics*, **118**, 166-181.

Shipilov, E.V., Lobkovsky, L.I., Shkarubo, S.I. and Kirillova, T.A. 2021. Tectono-Geodynamic Settings in the Conjugation Zone of the Lomonosov Ridge, Eurasian Basin, and Eurasian Continental Margin. *Geotectonics*, **55**, 655–675.

Smelror, M, Olaussen, S., Dumais, M.-A., Grundvåg, S.-A. and Abay, T.B. 2023. Northern Svalbard Composite Tectono-Sedimentary Element. Geological Society, London, Memoirs, https://doi.org/10.1144/M57-2023-2

Smith and Pickering 2003. Oceanic gateways as a critical factor to initiate icehouse Earth. *J Geol Soc*, **160**, 337-340.

Snow, J., Hellebrand, E., von der Handt, A., *et al*. 2011. Oblique nonvolcanic seafloor spreading in Lena Trough, Arctic Ocean. *Geochemistry, Geophysics, Geosystems*, **12**, doi:10.1029/2011GC003768

Sokolov, S.Yu., Geissler, W.H., Abramova, A.S., *et al*. 2023. Flat Spots within Cenozoic Sediments of the Nansen Basin, Arctic Ocean: Indicators for Serpentinization, Gas Generation and Accumulation Processes. *Lithology and Mineral Resources*, **58**, 1–15.

Speelman, E.N., van Kempen, M.M.L., Barke, J., *et al*. 2009. The Eocene Arctic Azolla bloom: environmental conditions, productivity and carbon drawdown. *Geobiology*, **7**, 155–170.

DOI: 10.1111/j.1472-4669.2009.00195.x

Stein, R., Jokat, W., Niessen, F. and Weigelt, E. 2015. Exploring the long-term Cenozoic Arctic Ocean climate history: a challenge within the International Ocean Discovery Program (IODP). *Arktos*, **1**, 1, 3.

Stein 2019. The late Mesozoic-Cenozoic Arctic Oceanclimate and sea ice history: A challenge for past and future scientific ocean drilling. *Paleocean Paleoclimat*, **34**

Stein, R. 2019b. The Expedition PS115/2 of the Research Vessel POLARSTERN to the Arctic Ocean in 2018. Reports on Polar and Marine Research, 72, 250 p.

Struijk, E.L.M., Tesauro, M., Lebedeva-Ivanova, N.N, et al. 2018. The Arctic lithosphere: Thermo-mechanical structure and effective elastic thickness. *Global and Planetary Change*, **171**, 2–17. https://doi.org/10.1016/j.gloplacha.2018.07.014

Sundvor, E., Eldholm, O., Gladczenko, T. and Planke, S. 2000. Norwegian-Greenland Sea thermal field. *Geological Society, London, Special Publications*, **167**, 397-410.

Urlaub, M., Schmidt-Aursch, M. C., Jokat, W. and Kaul, N. 2009. Gravity crustal models and heat flow measurements for the Eurasia Basin, Arctic Ocean. *Marine Geophysical Researches*, **30**, 277-292.

Vamvaka, A., Pross, J., Monien, P., Piepjohn, K., Estrada, S., Lisker, F. and Spiegel, C. 2019. Exhuming the top end of North America: Episodic evolution of the Eurekan belt and its potential relationships to North Atlantic plate tectonics and Arctic climate change. *Tectonics*, **38**, https://doi.org/10.1029/2019TC005621

Vanneste, M., Mienert, J. and Bünz, S. 2006. The Hinlopen Slide: A giant, submarine slope failure on the northern Svalbard margin, Arctic Ocean. *Earth and Planetary Science Letters*, **245**, 373–388. https://doi.org/10.1016/j.epsl.2006.02.045

Walker, J.D. and Geissman, J.W. (compilers) 2022. Geologic Time Scale v. 6.0: Geological Society of America, https://doi.org/10.1130/2022.CTS006C

Weigelt, E., Franke, D. and Jokat, W. 2014. Seismostratigraphy of the Siberian Arctic Ocean and adjacent Laptev Sea Shelf. *Journal of Geophysical Research: Solid Earth*, **119**, 5275–5289. https://doi.org/10.1002/2013JB010727

Weigelt, E., Jokat, W. and Eisermann, H. 2020. Deposition history and paleo-current activity on the southeastern Lomonosov Ridge and its Eurasian flank based on seismic data. *Geochemistry, Geophysics, Geosystems*, **21**, e2020GC009133. https://doi.org/10.1029/2020GC009133

Whaley, J. 2007. The Azolla Story: Climate Change and Arctic Hydrocarbons. *GEO ExPro*, **4**, 4.

Winkelmann, D., Geissler, W., Schneider, J. and Stein, R. 2008. Dynamics and timing of the Hinlopen/Yermak Megaslide north of Spitsbergen, Arctic Ocean. *Marine Geology*, **250**, 34–50. https://doi.org/10.1016/j.margeo.2007.11.013

Zayonchek, A.V., Mazarovich, A.O., Lavrushin, V.Yu., *et al.* 2009. Geological–Geophysical Studies in the Northern Barents Sea and on the Continental Shelf of the Arctic Ocean during Cruise 25 of the R/V Akademik Nikolay Strakhov. *Doklady Earth Sciences*, **427**, 740–745.

Zhang, X., Pease, V., Carter, A., *et al.* 2018. Timing of exhumation and deformation across the Taimyr fold–thrust belt: insights from apatite fission track dating and balanced cross-sections. *Geological Society, London, Special Publications*, **460**, 315–333.

Figure Captions

Figure 1: (A) Regional setting and location of study area. Topography and bathymetry from IBCAO (Jakobsson *et al.* 2020); (B) Main study area with outline of the Eurasia Basin Composite Tectono-Sedimentary Element (EB CTSE). Magnetic chrons based on Glebovsky et al. (2006a). Red stippled line shows the oceanic TSE and yellow stippled line shows the prograded margin TSE. Location of profiles in Figs. 4 and 5. FS, Fram Strait; FVT, Franz Victoria Trough; KT, Kvitøya Trough; LT, Lena Trough; MJR, Morris Jesup Rise; MS, Mosby Seamount; SB, Sophia Basin; ST, Starokadomsky Trough; StAT, St. Anna Trough; VT, Voronin Trough; YP, Yermak Plateau. 500 km and 250 km scale bars in black shown for A and B respectively.

Figure 2: Stratigraphic summary for the Eurasia Basin Composite Tectono-Sedimentary Element (EB CTSE) in relation to major tectonic and climatic events. Geological time scale from Walker and Geissman (2022). Tectono-Sedimentary Elements (TSE): EOB, Eurasia Oceanic Basin; EBPM, Eurasia Basin Prograded Margin; EARM CTSE, Eurasia Arctic Rifted Margin CTSE (Abdelmalak *et al.* 2024). Seismic stratigraphy: WNB, Western Nansen Basin (Engen *et al.* 2009; Lasabuda *et al.* 2018); EEB, Eastern Eurasia Basin (Nikishin *et al.* 2017); EAB, Eastern Amundsen Basin (Weigelt *et al.* 2020); WAB, Western Amundsen Basin (Castro *et al.* 2018). Stratigraphic summary for the ACEX borehole at the Lomonosov Ridge based on Backman *et al.* 2008. Average spreading rates for the Gakkel Ridge based on Glebovsky *et al.* 2006a. Also shown are tentative hydrocarbon play elements for the EB CTSE. See text for more details.

Figure 3: Geophysical and geological data covering the Eurasia Basin and surrounding areas. (A) Seismic reflection data (e.g. Weigelt *et al.* 2020; Nikishin *et al.* 2021; Funck *et al.* 2022), seismic refraction data (Jackson *et al.* 2010; Poselov *et al.* 2012; Drachev *et al.* 2018; Brotzer *et al.* 2022; Ding *et al.* 2022; Funck *et al.* 2022; Funck and Shimeld, 2023; Castro *et al.* 2024) and boreholes; (B) Other data: Shallow cores (Myhre *et al.* 1995; Backman *et al.* 2008; O'Regan, 2011) and seabed/dredged samples (Grantz *et al.* 2001; Poselov *et al.* 2012; Knudsen *et al.* 2018; Rekant *et al.* 2019); Heat flow data (Global Heat Flow Compilation 2013; Lucazeau 2019; heat flow values in mW m-2 shown for selected measurements); Some hydrothermal vents, pockmarks with gas discharge (Kristoffersen *et al.* 2022), flares (Blumenberg *et al.* 2016; Mau *et al.* 2017) and flat spots (Sokolov *et al.* 2023) also shown. KT, Kvitøya Trough; WVZ, Western Volcanic Zone (Gakkel Ridge).

Figure 4: Regional profiles across the Eurasia Basin. See Fig. 1B for location. Profile A is based on Shipilov *et al.* (2021); Profile B is based on Nikishin *et al.* (2017) and Shipilov *et al.* (2021); Profile C is based on Jokat *et al.* (1995b), Jokat and Micksch (2004), Engen *et al.* (2009), Castro *et al.* (2018), and

Lasabuda *et al.* (2018); Profile D is based on Jokat *et al.* (1995a). Location of magnetic chrons are shown along the profiles (for ages see Fig. 2). BS, Barents Sea; ESS, East Siberian Shelf; GR, Gakkel Ridge; KS, Kara Sea; LR, Lomonosov Ridge; LS, Laptev Sea; MJR, Morris Jesup Rise; YP, Yermak Plateau.

Figure 5: Seismic profiles across the conjugate Lomonsov Ridge and northern Barents Sea margins reaching chron 22 in both the Amundsen and Nansen basins. See Fig. 1B for location of profiles. Location of magnetic chrons are shown along both profiles (for ages see Fig. 2). The profile in (A) was first published by Funck *et al.* (2022). Based on integration of results from seismic reflection and refraction data they proposed three crustal domains: (1) thin continental crust down-faulted from the main Lomonosov Ridge; (2) exhumed and serpentinized mantle with some gabbroic intrusions; and (3) oceanic crust. The profile in (B) is located close to a similar profile published by Lutz *et al.* (2018). A similar sub-division into crustal domains is tentatively shown for this profile also.

Figure 6: (A) Present-day simplified geological map. Magnetic chrons based on Glebovsky *et al.* (2006a); (B) Plate reconstructions to chron 13 in the earliest Oligocene; (C) Plate reconstruction to chron 24 in the earliest Eocene - corresponding to breakup. SB, Sophia Basin.

Figure 7: Sediment thickness maps. (A) Total sedimentary thickness (based on Døssing *et al.* 2014; Nikishin *et al.* 2021; Rekant *et al.* 2021). Thicknesses are also shown outside the Eurasia Basin CTSE and here the map mainly covers pre-Cenozoic strata. (B) Thickness of glacial sediments forming large fans deposited in front of bathymetric troughs on the Barents-Kara shelf (Hjelstuen and Sejrup 2021). FVT, Franz Victoria Trough; ST, Starokadomsky Trough; StAT, St. Anna Trough; VT, Voronin Trough.

Table Caption

Table 1: Key references for seismic stratigraphic framework of different areas/provinces in the Eurasia Basin (see Fig. 1B for location).

Area	References
Western Nansen Basin	Jokat et al. 1995a; Geissler and Jokat 2004; Engen *et al.* 2009; Berglar *et al.* 2016; Lasabuda *et al.* 2018
Western Amundsen Basin	Jokat *et al.* 1995b; Castro *et al.* 2018
Central Amundsen Basin	Jokat *et al.* 1995b; Cernykh and Krylov 2011
Eastern Amundsen Basin	Weigelt *et al.* 2014, 2020; Nikishin *et al.* 2017, 2018
Russian Eurasia Basin	Shipilov *et al.* 2020; Nikishin *et al.* 2021a,b; Rekant *et al.* 2021
Yermak Plateau	Geissler *et al.* 2011; Kristoffersen *et al.* 2020
Sophia Basin	Geissler and Jokat 2004; Geissler *et al.* 2011
Morris Jesup Rise	Kristoffersen *et al.* 2021
Fram Strait/Lena Trough	Geissler et al. 2011; Mattingsdal *et al.* 2014

Table 1

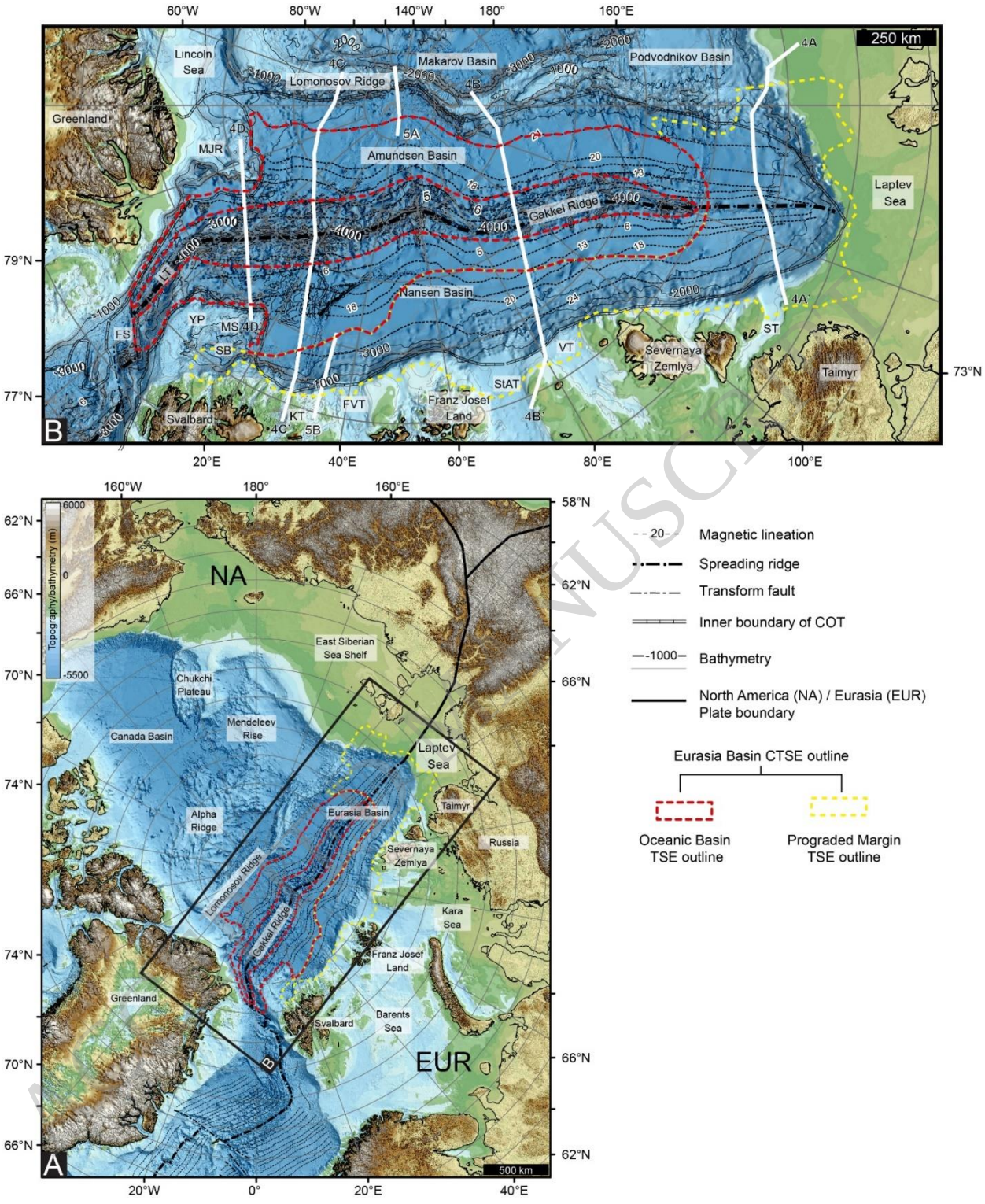
60°W
80°W
140°W
180°
160°E
250 km
Lincoln Sea
Greenland
Lomonosov Ridge
Makarov Basin
Podvodnikov Basin
4A
4C
4B
4D
5A
MJR
Amundsen Basin
Laptev Sea
Gakkel Ridge
79°N
LT
YP
MS
FS
SB
Nansen Basin
VT
ST
Severnaya Zemlya
Taimyr
73°N
77°N
StAT
FVT
KT
5B
Franz Josef Land
Svalbard
B
20°E
40°E
60°E
80°E
100°E
160°W
180°
160°E
62°N
66°N
70°N
74°N
58°N
NA
Topography/bathymetry (m)
6000
0
-5500
East Siberian Sea Shelf
Chukchi Plateau
Mendeleev Rise
Canada Basin
Laptev Sea
Alpha Ridge
Eurasia Basin
Taimyr
Russia
Severnaya Zemlya
Lomonosov Ridge
Gakkel Ridge
Kara Sea
Franz Josef Land
Greenland
Svalbard
Barents Sea
EUR
A
500 km
20°W
0°
20°E
40°E
Magnetic lineation
Spreading ridge
Transform fault
Inner boundary of COT
Bathymetry
North America (NA) / Eurasia (EUR) Plate boundary
Eurasia Basin CTSE outline
Oceanic Basin TSE outline
Prograded Margin TSE outline

Figure 1

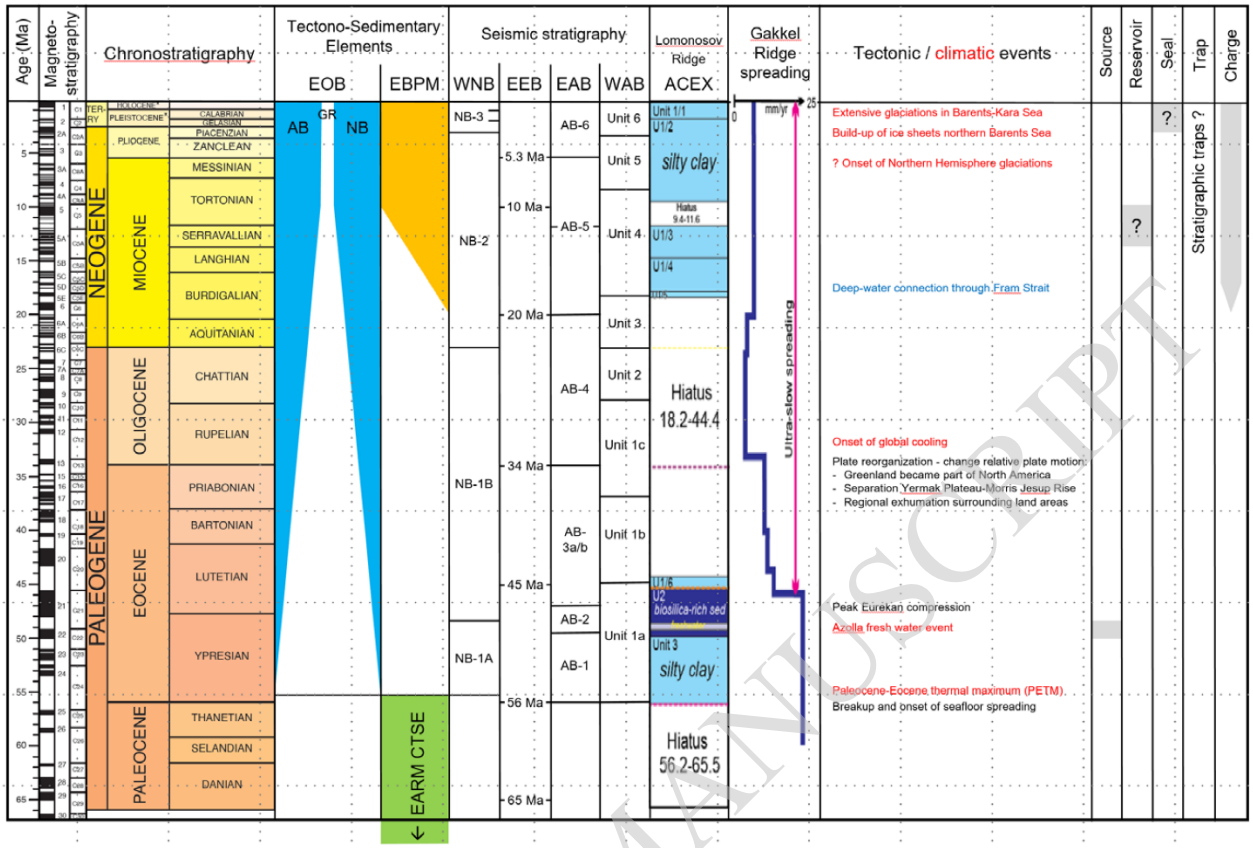

Figure 2

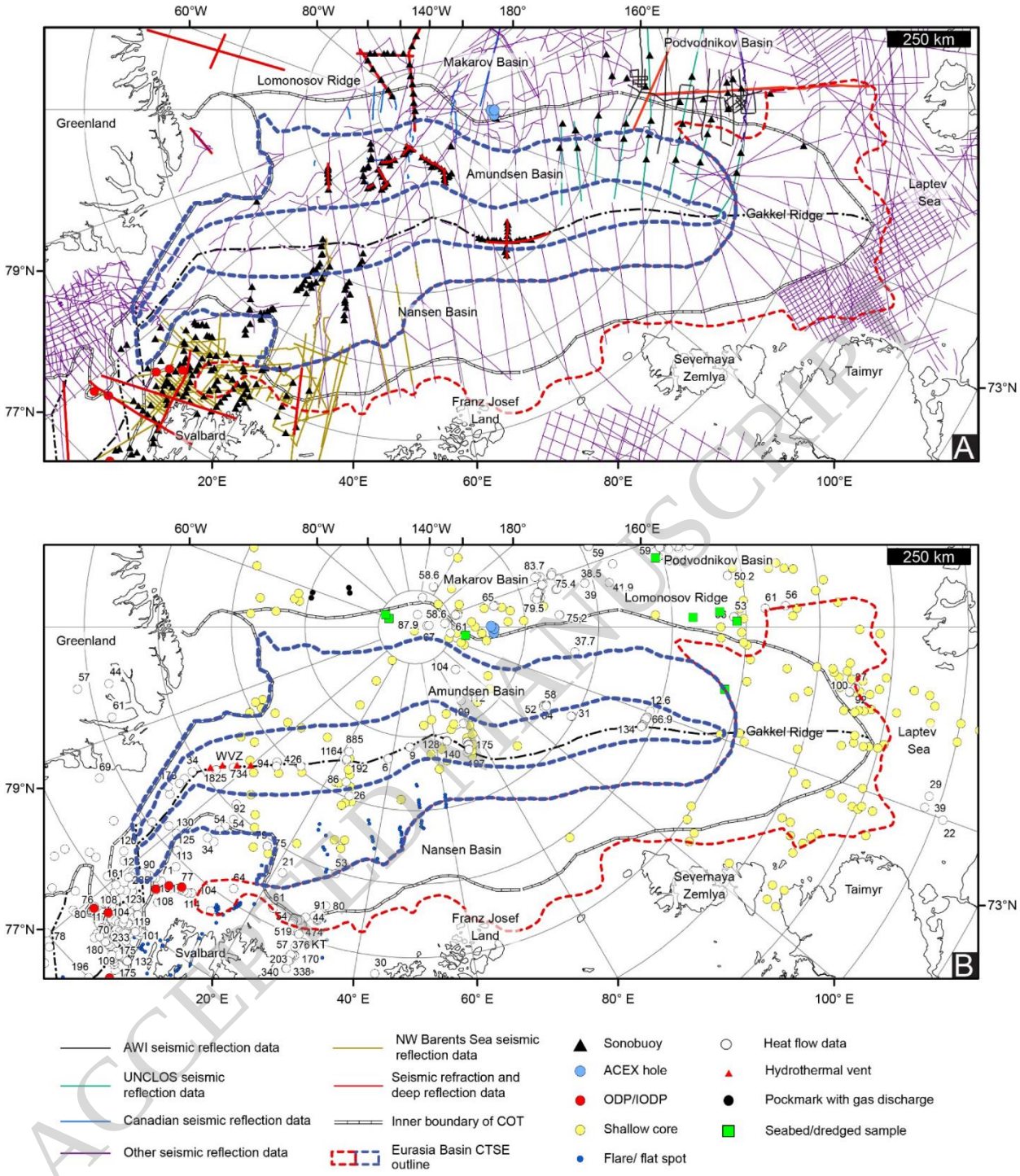

Figure 3

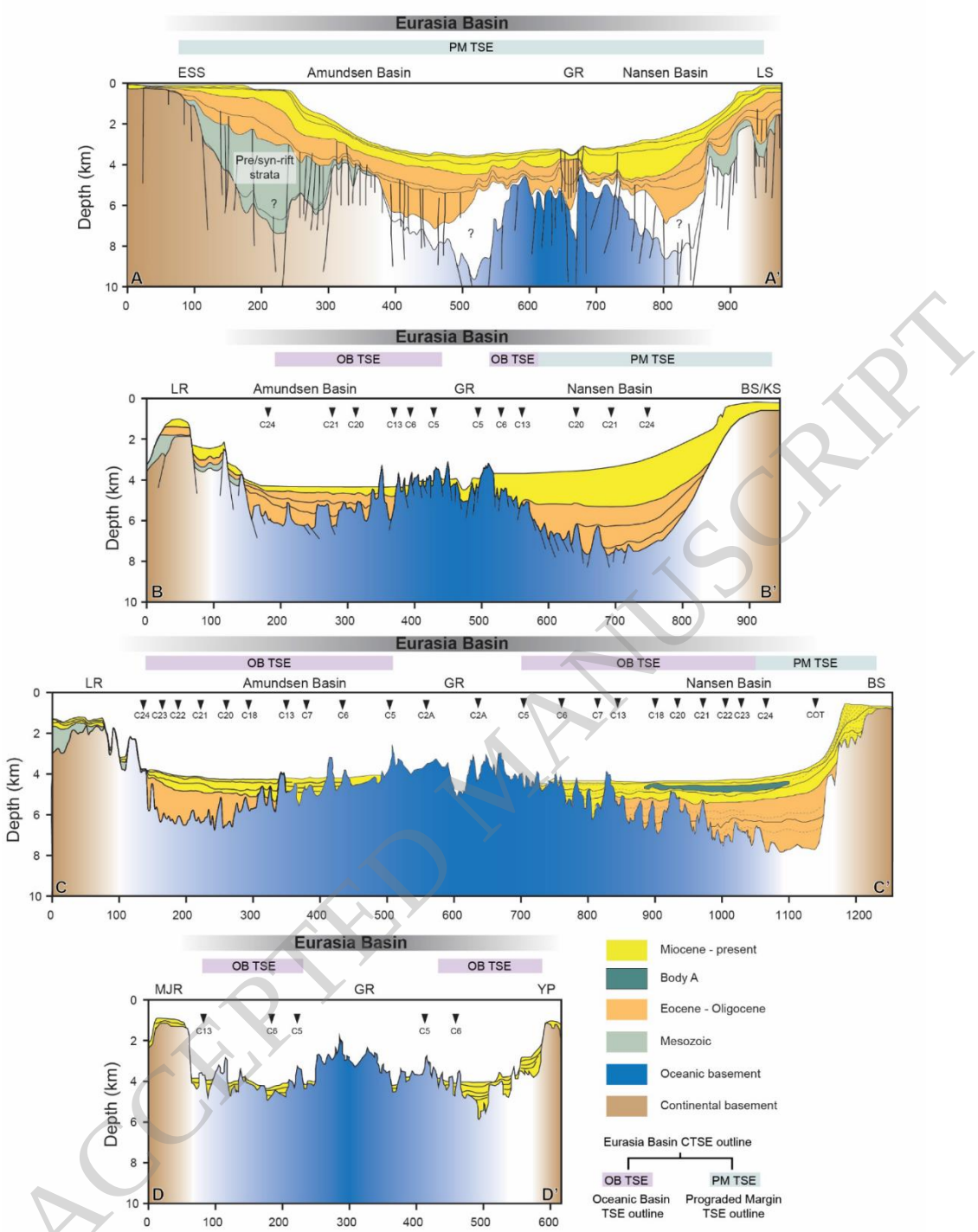

Figure 4

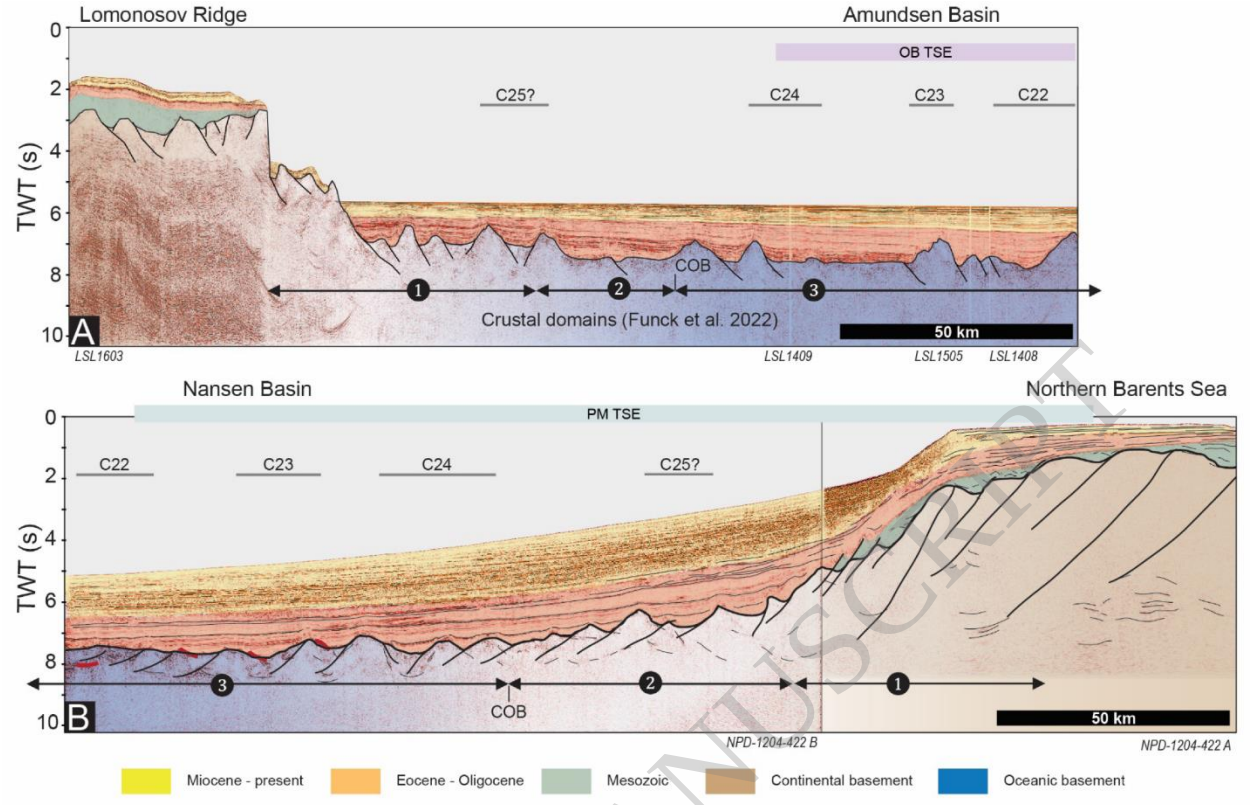

Figure 5

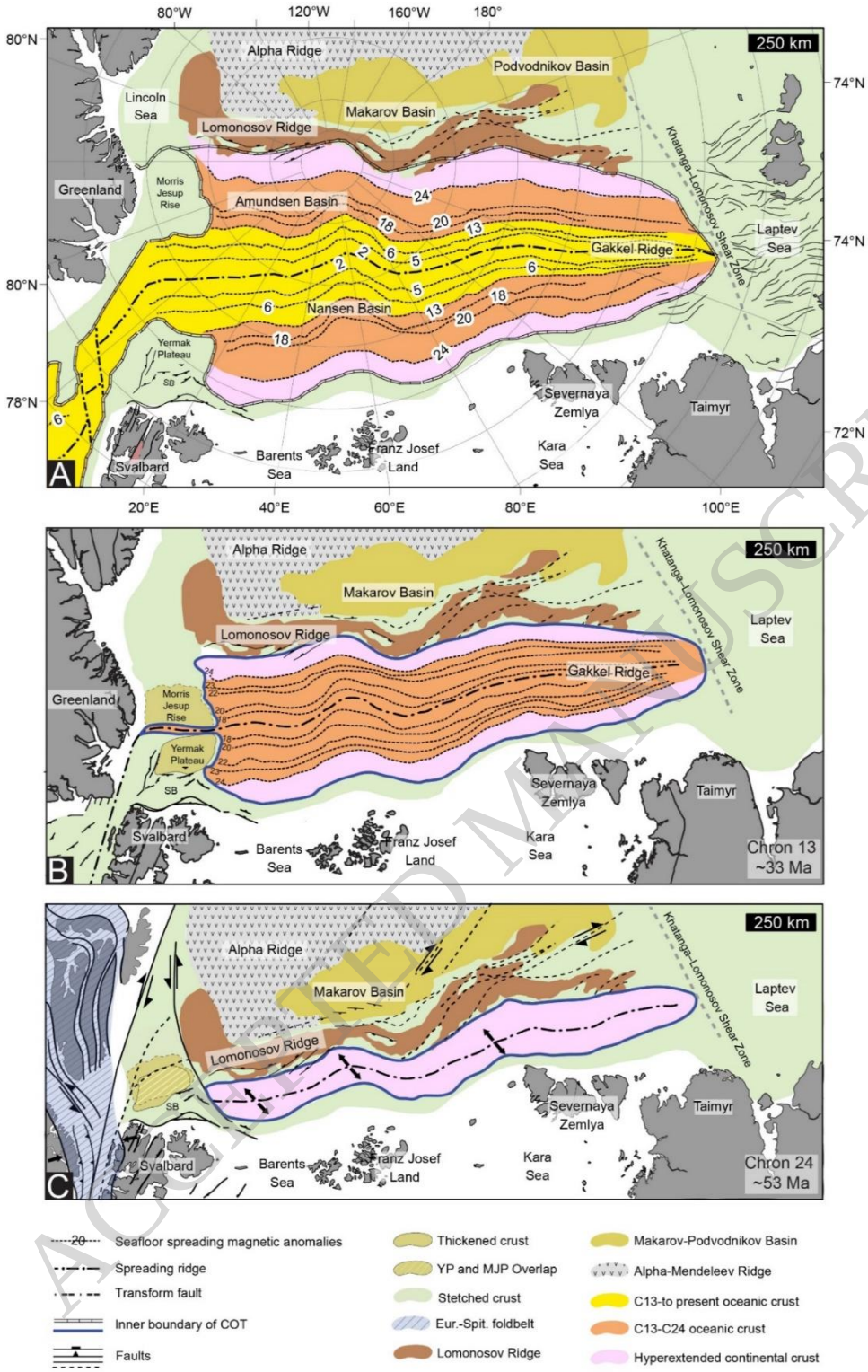

Figure 6

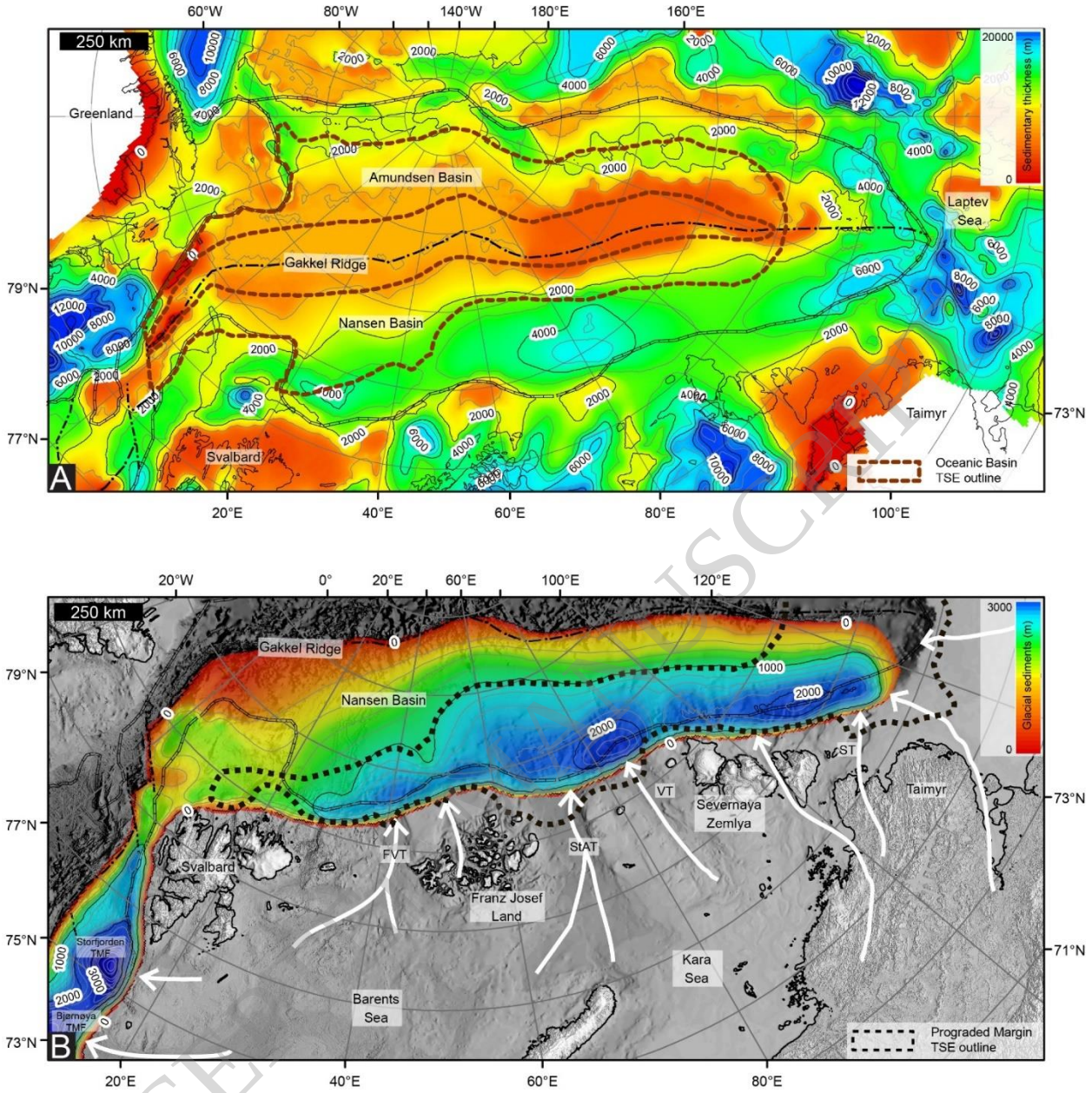
60°W
80°W
140°W
180°E
160°E
250 km
Greenland
Amundsen Basin
Gakkel Ridge
Nansen Basin
Laptev Sea
Taimyr
Svalbard
Oceanic Basin TSE outline
Sedimentary thickness (m)
20000
0
79°N
77°N
73°N
20°E
40°E
60°E
80°E
100°E
A
20°W
0°
20°E
60°E
100°E
120°E
250 km
Gakkel Ridge
Nansen Basin
Svalbard
FVT
StAT
VT
ST
Severnaya Zemlya
Taimyr
Franz Josef Land
Storfjorden TMF
Bjørnøya TMF
Barents Sea
Kara Sea
Prograded Margin TSE outline
Glacial sediments (m)
3000
0
79°N
77°N
75°N
73°N
71°N
20°E
40°E
60°E
80°E
B

Figure 7